THE JOURNAL OF COMPARATIVE NEUROLOGY 451:153–169 (2002)

Role of *Emx2* in the Development of the Reciprocal Connectivity Between Cortex and Thalamus

GUILLERMINA LÓPEZ-BENDITO,[1] CHUN-HUNG CHAN,[2,3]
ANTONELLO MALLAMACI,[4] JOHN PARNAVELAS,[2] AND ZOLTÁN MOLNÁR[1]*
[1]Department of Human Anatomy and Genetics, University of Oxford, Oxford, OX1 3QX, United Kingdom
[2]Department of Anatomy and Developmental Biology, University College London, London, WC1E 6BT, United Kingdom
[3]Center for Aging and Developmental Biology, University of Rochester Medical Center, Rochester, New York 14642
[4]Department of Biological and Technological Research (DIBIT), Istituto Scientifico H. San Raffaele, 20132 Milan, Italy

ABSTRACT

Emx2 knockout mice appear to show a shift in the areal identity in the cerebral cortex of *Emx2* knockout mice, which is matched with altered distribution of thalamocortical projections (Bishop et al. [2000] Science 288:344–3349; Mallamaci et al. [2000] Nat Neurosci. 3:679–686). We have examined the early establishment of these projections to understand how the altered *Emx2* expression results in changes in their cortical targeting. We used carbocyanine dye tracing to visualize thalamocortical and corticofugal projections as well as immunohistochemistry for L1 and TAG-1, respective markers of the two axonal systems, in wild-type, heterozygote, and null mutant for *Emx2* at embryonic (E) ages ranging from E13.5 to E18.5. These tracing studies demonstrated that, in *Emx2* knockout mice, a large proportion of early thalamocortical projections were misrouted at the border between the diencephalon and telencephalon. This abnormality was associated with displaced connectivity of the internal capsule cells at the diencephalic–telencephalic junction. Interestingly, most of the aberrant thalamic projections compensated for the ventral entry to the telencephalon and still ascended to the cortex. Although this early targeting abnormality is associated with the altered *Emx2* expression pattern in the cortex, it most probably occurs independently from it, and is related to earlier guidance defects at the diencephalic–telencephalic boundary. These defects might result in the altered and delayed arrival of thalamic projections to the cortex and, thus, contribute to the shifted thalamocortical matching previously observed in the *Emx2* knockout mice. J. Comp. Neurol. 451:153–169, 2002. © 2002 Wiley-Liss, Inc.

Indexing terms: L1; TAG-1; mouse; carbocyanine dyes; immunohistochemistry

The early pattern of development of thalamocortical connections follows a similar sequence in all mammals. Axons descend through the ventral thalamus, advance among cells in the internal capsule, which already possess dorsal thalamic projections, then reach the cerebral cortex by associating with subplate cells and their early corticofugal projections (Molnár et al., 1998a). Selective fasciculation, contact guidance, release of neurotrophic factors, gradients of cortical gene expression, and early neuronal activity are thought to play important roles in the development of thalamocortical projections (Bolz et al., 1993; Allendoerfer and Shatz, 1994; Molnár and Blakemore, 1995; Catalano and Shatz, 1998). During their growth, thalamic fibers cross gene expression boundaries, both within the diencephalon and telencephalon. On these occasions, their fasciculation pattern and growth kinetics change. It has been described that thalamic projections

Grant sponsor: The Royal Society, Swiss National Science Foundation; Grant number: 3100-56032.98; Grant sponsor: European Community; Grant number: QLRT-1999-30158; Grant number: QLG3-CT-2000-00158; Grant sponsor: The Welcome Trust; Grant number: 063974/B/01/Z; Grant sponsor: St John's College, Oxford.

*Correspondence to: Zoltán Molnár, Department of Human Anatomy and Genetics, University of Oxford, South Parks Road, Oxford, OX1 3QX, UK. E-mail: zoltan.molnar@anat.ox.ac.uk

Received 20 November 2001; Revised 20 March 2002; Accepted 7 June 2002
DOI 10.1002/cne.10345

© 2002 WILEY-LISS, INC.

initially pause in the internal capsule and then pause again in the subplate layer before entering the cortical anlage (Rakic, 1977; Métin and Godement, 1996). The interactions of the thalamocortical projections with the early generated, largely transient cells of the ventral thalamus, internal capsule, and subplate are believed to play a crucial role in the deployment of thalamic projections through the various regions of the developing forebrain (Blakemore and Molnár, 1990; Molnár and Cordery, 1999). Altered gene expression patterns along the thalamocortical path can arrest or modify their development. There seem to be at least two especially critical zones in the embryonic forebrain, where thalamic projections become altered in homeobox gene knockout mice. One critical zone is at the telencephalon–diencephalon border, and the other is at the corticostriatal junction (Molnár and Butler, 2002). Hevner et al. (1998, 2001) and Kawano et al. (1999) have described errors occurring in corticothalamic and thalamocortical pathfinding within the region of the internal capsule in mice with mutations of transcription factor genes expressed in cortex (*Tbr1*), dorsal thalamus (*Gbx2*), or in both (*Pax6*). Impairment in the early growth of thalamic axons in *Mash1* and *Sema6A* knockout mice has already been reported (Tuttle et al., 1999; Leighton et al., 2001). The disturbed thalamocortical development in transgenic mice, including *Emx2* knockout mice, might be a very sensitive indicator of the disturbed early regionalization and the consequences of altered forebrain development.

Emx2 is a member of the empty spiracles family of genes, and its expression in the anterior central nervous system of the developing mouse embryo follows a rostrocaudal gradient (Simeone et al., 1992a,b; Gulisano et al., 1996; Mallamaci et al., 1998; Bishop et al., 2000). Homozygous mutant mice for *Emx2* die perinatally, probably due to the absence of kidneys. Previous studies have shown that the lack of *Emx2* results in some forebrain structure abnormalities. The most striking abnormalities are the severe reduction of cortical hemisphere size and the disruption in cortical lamination (Yoshida et al., 1997; Mallamaci et al., 2000a). The archicortex of these animals is also heavily affected. The dentate gyrus cannot be readily identified; however, the dentate cells can be revealed with molecular markers (Tole et al., 2000). The hippocampus and the medial limbic cortex are greatly reduced in size. Lamination defects have been reported to occur in the neocortex of *Emx2* knockout mice (Pellegrini et al., 1996; Yoshida et al., 1997; Mallamaci et al, 2000a), but the diencephalon develops relatively normally (Suda et al., 2001). A disproportional, but orderly, arealization of the *Emx2* mutant neocortex reflected by an expansion of rostral areas and a contraction of caudal areas has been described (Bishop et al., 2000; Mallamaci et al., 2000b). This shift in areal identity in the cerebral cortex of *Emx2* knockout mice is matched by the altered distribution of thalamocortical projections. This finding led to the proposal that shifts in cortical *Emx2* and *Pax6* expression gradients might be responsible for arealization and altered thalamocortical connectivity (Bishop et al., 2000; Mallamaci et al., 2000b). To understand how the altered *Emx2* expression results in changed cortical targeting, we examined the early *Emx2* expression along the path of thalamic axons, and systematically documented the establishment of thalamocortical and corticothalamic patterns, before and during the time these projections reach the cortex. We specifically tested the idea of whether thalamocortical axons become misrouted close to the start of their path toward the cortex, where cues other than the ones intrinsic to the cortex could influence their behavior.

MATERIALS AND METHODS

Genotyping of *Emx2* embryos

Screening of embryonic mice was carried out by coamplification of DNA fragments corresponding to the wild-type (WT) and mutant *Emx2* gene sequences. To achieve this coamplification, one forward primer was used for both WT and mutant amplification, but two different primers, corresponding to the WT and mutant gene sequences, were used. The primer sequences used were as follows:

*Emx2*F 5′ CAC AAG TCC CGA GAG TTT CCT TTT GCA CAA CG 3′

*Emx2*R/WT 5′ ACC TGA GTT TCC GTA AGA CTG AGA CTG TGA GC 3′

*Emx2*R/KO 5′ ACT TCC TGA CTA GGG GAG GAG TAG AAG GTG G 3′

Genomic DNA was isolated from tissue samples obtained from the embryos and subjected to polymerase chain reaction (PCR) amplification (98°C for 5 minutes; 98°C for 1 minute, 72°C for 2 minutes, 5×; 94°C for 1 minute, 72°C for 2 minutes, 30×; 72°C for 10 minutes) by using a thermocycler (Hybaid). PCR products were analyzed by gel electrophoresis through a 2% agarose gel. Care and handling of animals prior to and during experimental procedures followed Home Office U.K. regulations.

Tracing with carbocyanine dyes

Twelve pregnant C57/B16 mice were used for the study. Timed pregnant females were killed by deep ether anesthesia followed by cervical dislocation. Fetuses were harvested by caesarean section. Embryonic brains were dissected and fixed in 4% paraformaldehyde in 0.1 M phosphate buffer (PB, pH 7.4) overnight. To label thalamic and corticofugal fibers, small holes were made with a stainless steel electrode into the dorsal thalamus and the cerebral cortex of both hemispheres of each brain, and single crystals of 1,1′-dioctadecyl-3,3,3′,3′-tetramethylindocarbocyanine perchlorate (DiI) and 4-(4-(dihexadecylamino) styryl)-*N*-methylpyridinium iodide (DiA) (Molecular Probes, Leiden, The Netherlands) were placed into them by using the same electrodes under a binocular dissecting microscope (Godement et al., 1987; Molnár et al., 1998a). We examined E13.5: n = 4 $Emx2^{+/+}$, n = 4 $Emx2^{-/-}$; E14.5: n = 4 $Emx2^{+/+}$, n = 2 $Emx2^{+/-}$, n = 4 $Emx2^{-/-}$; E15.5: n = 6 $Emx2^{+/+}$, n = 4 $Emx2^{+/-}$, n = 6 $Emx2^{-/-}$; E17.5: n = 4 $Emx2^{+/+}$, n = 2 $Emx2^{+/-}$, n = 6 $Emx2^{-/-}$; E18.5: n = 8 $Emx2^{+/+}$, n = 2 $Emx2^{+/-}$, n = 8 $Emx2^{-/-}$ hemispheres. At E16.5, we further examined n = 4 $Emx2^{-/-}$ and n = 6 $Emx2^{+/+}$ hemispheres, and at E18.5, n = 3 $Emx2^{-/-}$ and n = 3 $Emx2^{+/+}$ brains with ventral telencephalic crystal placements to identify the source of the fibers surfacing to the ventral telencephalon at the junction of the diencephalon and telencephalon. For these experiments, both hemispheres were used.

Specimens were kept in 2% paraformaldehyde for 2 weeks at room temperature in the dark. Because the incubation period of DiA is slightly shorter than DiI, we used delayed DiA implantation (in general after 7 days of DiI incubation). Brains were then washed in PBS (pH 7.4), embedded into 4% agarose (Sigma) and cut at 100 μm with

a Vibroslice (Leica, VT1000S). Sections were counterstained with 2.5 μg/ml of bisbenzamide (Sigma), mounted in PBS/glycerol onto slides, and analyzed by using an epifluorescence microscope (Leica, DMR) and a laser scanning confocal microscope (Leica, DMRE).

Histochemistry and immunohistochemistry

Hematoxylin staining was performed on 70% ethanol-5% acetic acid–fixed, wax-embedded brains, from E15.5 *Emx2*$^{+/+}$ (n = 2) and *Emx2*$^{-/-}$ (n = 2) embryos, according to standard methods. A polyclonal antibody against L1 (used 1:100, Roche Diagnostics) and a monoclonal antibody against TAG-1 (4D7, we used 1:100, Developmental Hybridoma Bank, Iowa City, IA, for details, see Denaxa et al., 2001), were used in WT (*Emx2*$^{+/+}$), heterozygote (*Emx2*$^{+/-}$), and null mutants (*Emx2*$^{-/-}$) at E14.5, E15.5, 16.5, and E17.5 (three brains for each stage) and one brain for E13.5. Brains were fixed in 4% paraformaldehyde in 0.1 M PB, embedded into low melting agarose (Sigma, 5% in 0.1 M PB), and cut with Vibroslice at 60 μm. Standard immunohistochemical procedures were applied on free-floating sections. For L1 antibody, immunohistochemistry was performed on wax-embedded sections (10 μm). EMX2 immunohistochemistry was performed on methanol/dimethyl sulfoxide (4:1) -fixed, wax-embedded sections of E13.5, E16.5 WT brains as described by Mallamaci et al. (1998). Results were documented with a Leica DC 500 digital camera, and figures were produced using Adobe Photoshop.

RESULTS

EMX2 immunohistochemistry and hematoxylin staining

Analysis of the distribution of the EMX2 in WT E13.5 and E16.5 brains confirmed the previous report of the graded expression of this homeoprotein in the ventricular zone of the developing cortex, with a medial maximum and a lateral minimum (Mallamaci et al., 1998). In addition, it revealed numerous EMX2-immunoreactive cells in the marginal part of the ventral telencephalon as well as in the diencephalon, at the boundary between thalamus and hypothalamus (Fig. 1A–D,G). In some sections, these cells seemed to form a continuous group extending from diencephalon to telencephalon (Fig. 1C,D).

Hematoxylin staining of E15.5 WT (Fig. 1E,H) and *Emx2* null mutant brains (Fig. 1F,I) provided useful information on the cytoarchitectural differences between the two groups. In WT brains, the internal capsule is noticeable due to its cell free nature. In *Emx2*$^{-/-}$, two areas showing a distinct paucity of cells were noted. One at the marginal edge of the ventral telencephalon and one at the junction between diencephalon and telencephalon, both presumably correspond to accumulations of disorganized thalamic fibers (Fig. 1F,I).

Carbocyanine dye tracing

Thalamic crystal placements. In both *Emx2*$^{+/+}$ and *Emx2*$^{+/-}$ E15.5 mice, dorsal thalamic carbocyanine crystal placements revealed that thalamic axons descend from dorsal thalamus (DT) through the ventral thalamus, where they turn laterally to enter the internal capsule (Fig. 2A). The axons arrive in the intermediate zone (IZ) of the cortex where they extend parallel to the cortical surface (Fig. 2E). However, in *Emx2*$^{-/-}$ mice, a large proportion of the thalamic projections continued to descend to the basal telencephalon and extend ventrally at the junction of the diencephalon with the telencephalon, rather

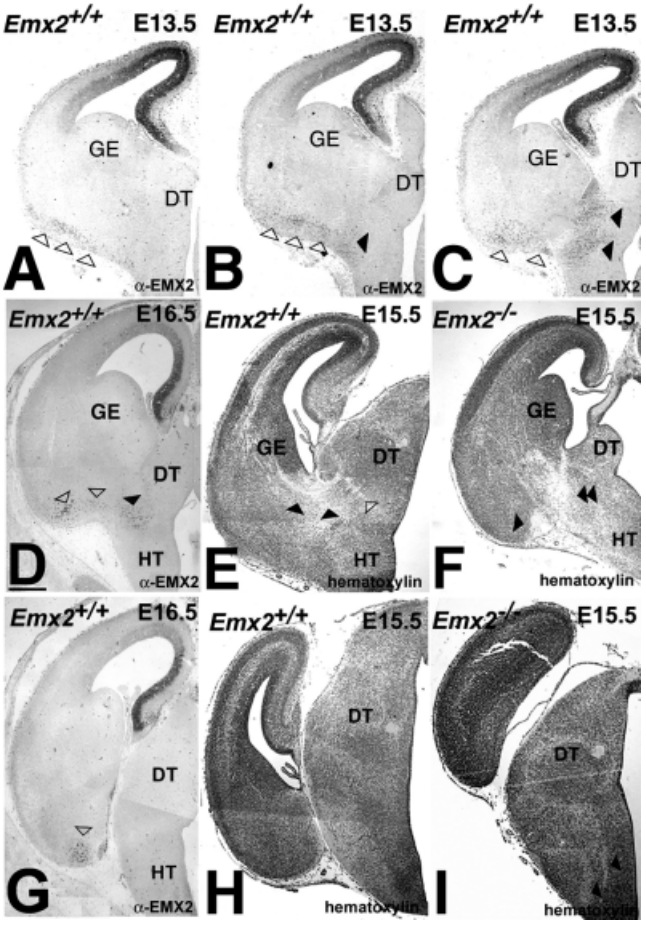

Fig. 1. Distribution of EMX2 immunoreactivity in an embryonic day (E) 13.5 wild-type (WT; A–C), E16.5 WT (D,G), and the gross appearance of hematoxylin-stained sections of E15.5 WT (E,H) and *Emx2*$^{-/-}$ (F,I) brains. **A–C:** Distribution of the EMX2 homeoprotein in frontal sections at three rostrocaudal levels from a WT E13.5 brain as revealed by a polyclonal α-EMX2 antiserum. EMX2 is detectable in the ventricular zone of the developing cortex, where its expression is graded with a medial maximum and a lateral minimum. Numerous EMX2-immunoreactive cells are clustered at the margin of the ventromedial telencephalon (open arrowheads), as well as at the boundary between dorsal thalamus (DT) and hypothalamus (HT) (solid arrowheads). **D,G:** At E16.5, EMX2 expression is maintained in the ventral telencephalon (open arrowheads) and in the diencephalon–telencephalon junction (solid arrowheads). **E,F,H,I:** Hematoxylin staining of frontal sections from E15.5 WT (E,H) and *Emx2* null mutant brains (F,I). A cell-poor, fan-shaped area can be seen at the diencephalic–telencephalic junction of the WT brain corresponding to regularly arranged axon bundles connecting cortex and thalamus (solid arrowheads in E). In the *Emx2* mutant brain, two areas with low cell density can be detected. One area is located at the ventral-marginal edge of the telencephalon (single arrowhead in F). The second region was found at the diencephalon–telencephalon junction (double arrowhead in F). Both of these areas presumptively corresponded to accumulative fibers. Note also the cell-poor area corresponding to misrouted axon bundles extending to the hypothalamic region (arrowheads in I) not seen in WT brains (H). The boundary between the dorsal and ventral thalamus (open arrowhead at E) is not apparent in the *Emx2*$^{-/-}$ brains (F). GE, ganglionic eminences. Scale bar = 200 μm in D (applies to A–I).

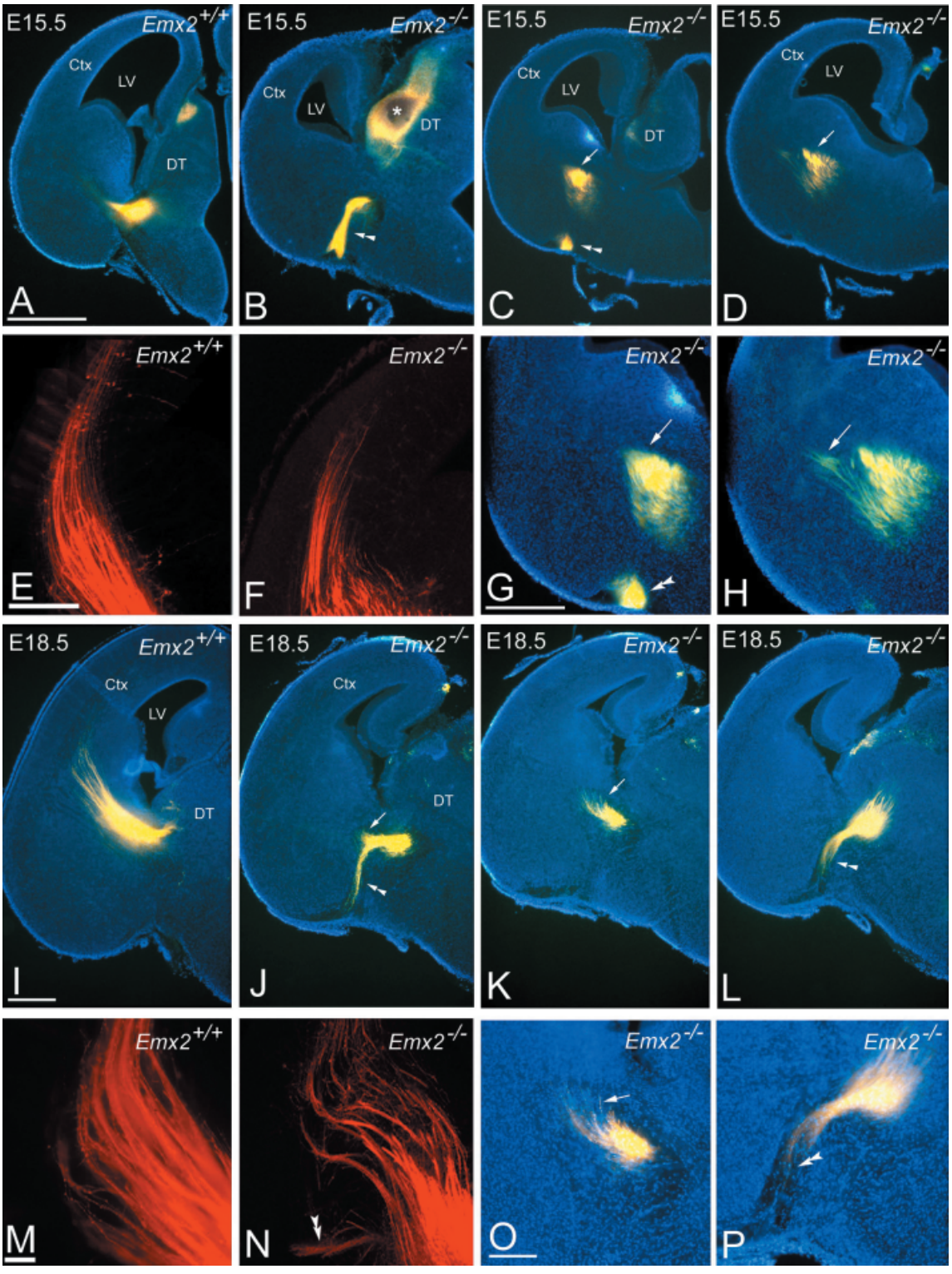
E15.5
Emx2+/+
Ctx
LV
DT
A
E15.5
Emx2-/-
Ctx
LV
*
DT
B
E15.5
Emx2-/-
Ctx
LV
DT
C
E15.5
Emx2-/-
Ctx
LV
D
Emx2+/+
E
Emx2-/-
F
Emx2-/-
G
Emx2-/-
H
E18.5
Emx2+/+
Ctx
LV
DT
I
E18.5
Emx2-/-
Ctx
DT
J
E18.5
Emx2-/-
K
E18.5
Emx2-/-
L
Emx2+/+
M
Emx2-/-
N
Emx2-/-
O
Emx2-/-
P

Figure 2

than turning laterally to enter the internal capsule (Fig. 2B). Nevertheless, some thalamic fibers in the mutant did reach the cortex as well (Fig. 2F). Approximately half of the labeled fibers descended into the ventral telencephalon, and the other half followed the normal developmental pattern (Fig. 2C). The misrouted axons at the ventral segment of the telencephalon–diencephalon junction turned dorsally toward the internal capsule (Figs. 3F, 4F).

By E18.5, thalamic projections reached most parts of the dorsal cortex and the fibers accumulated below the cortical plate in normal and heterozygous mice (Fig. 2I,M). However, in the $Emx2^{-/-}$ hemispheres, the labeled thalamic fibers were again split into two groups at the medial part of the internal capsule (Fig. 2J). Approximately half of the labeled fibers descended into the ventral telencephalon and surfaced at the telencephalon and diencephalon border (Fig. 2L,P). The other half of the fibers followed a normal developmental pattern entering the internal capsule and extending toward the cortex (Fig. 2K,O). Also, the majority of mutants had a disorganized pattern of thalamic fiber fascicles in the internal capsule (Fig. 2N).

It has been described that both dorsal and ventral thalamic crystal placements label a group of cells within the internal capsule (Métin and Godement, 1996; Molnár and Cordery, 1999). With early thalamic projections, these cells are situated within and around the primitive internal capsule and below both the lateral and medial ganglionic eminences. In both $Emx2^{+/+}$ and $Emx2^{-/-}$ E13.5 and E15.5 mice, placement of carbocyanine crystals in the dorsal thalamus revealed a large number of backlabeled cells within and around the internal capsule and within the anlage of the striatum (Figs. 3A,F, 4A,B). In the $Emx2^{-/-}$ brains, some of the backlabeled cells were displaced ventrally in the telencephalon near the telencephalic-diencephalic border (Fig. 4B,D). Their position corresponded to the ventrally displaced fiber bundle (Fig. 4B,E). From these ventrally displaced fiber bundles, axons ascended toward cells in more dorsal parts of the internal capsule (Figs. 3F, 4E,F). At E13.5, carbocyanine dye tracing and TAG-1 immunohistochemistry revealed that the early corticofugal projections left the cortex in both $Emx2^{+/+}$ and $Emx2^{-/-}$ brains (Fig. 3B,H,D,J), but in the mutant, they extended along more superficial sector of the cortex and their front reached the lateral part of the internal capsule more widespread (Fig. 3I).

Ventral telencephalic crystal placements. To identify the specific origin of the dorsal thalamic projections that were derailed to the ventral telencephalon in the *Emx2* mutant, DiI crystals were placed into the junction of the telencephalon and the diencephalon (Fig. 5, first panel). For these experiments, four E15.5 $Emx2^{-/-}$ brains and six $Emx2^{+/+}$ control brains, and for later ages, three E18.5 $Emx2^{-/-}$ brains and three $Emx2^{+/+}$ control brains were used. We were particularly interested in the possibility that the derailed fibers may originate from a specific region of the dorsal thalamus. Indeed, DiI crystal placements at the ventral part of the telencephalic-diencephalic border of E15.5 brains revealed more backlabeled cells in the ventromedial aspect of thalamus in the *Emx2* mutant mice compared with E15.5 WT (Fig. 5A,B and C,D, respectively). At E18.5, the difference between the number and distribution of the labeled cells in the dorsal thalamus of the WT and mutant was even more apparent (Fig. 5E–H). At both ages, in WT brains, such DiI placements revealed backlabeled cells in the cortical plate of the entorhinal cortex (Fig. 5I,J). It is known that entorhinal cortex sends projections to the amygdala and also that projections from the neighboring perirhinal cortex are among the first to cross the ventral part of the primitive internal capsule (see Molnár and Cordery, 1999). Both projections could have been backlabeled from the DiI crystal placements into the diencephalon–telencephalon junction. In $Emx2^{-/-}$ brains, the backlabeled cells were disorganized and located in the entorhinal cortex (Fig. 5K,L). Unlike the WT dendrites that organize perpendicularly to the pial surface (Fig. 5I,J), the mutant dendrites are dispersed with various orientations (Fig. 5K,L).

Cortical crystal placements. To reveal the descending corticofugal projections at different ages, single carbocyanine crystals were placed into the dorsal cortex of $Emx2^{+/+}$ and $Emx2^{-/-}$ mice. At E13.5 and E15.5, cortical crystal placements in $Emx2^{+/+}$ and $Emx2^{+/-}$ revealed the first corticofugal projections descending through the intermediate zone (IZ) to the striatocortical junction, where most of them lined up and paused (Fig. 3). In the $Emx2^{-/-}$ mice, despite the more superficial position in cortex and wider dispersion at the striatocortical junction (Fig. 3H) the majority of the corticofugal projections acquired the normal pattern, with the exception of the most lateral and superficial cortical projections, which did not turn medially, but rather continued to extend ventrally toward the ventrolateral pallium (see Fig. 8C,D). This pattern was also observed in E16.5 hemispheres. How-

Fig. 2. Early targeting error of thalamic projections in the $Emx2^{-/-}$ mice at the diencephalon–telencephalon junction. Thalamic fibers labeled with 1,1′-dioctadecyl-3,3,3′,3′-tetramethylindocarbocyanine perchlorate (DiI) crystals placed into the dorsolateral part of the left thalamus of wild-type (WT; A,E,I,M) and mutant $Emx2^{-/-}$ mice (B–D,F–H,J–L,N–P) at embryonic day (E) 15.5 (A–H) and E18.5 (I–P). After 2 weeks of incubation at room temperature, 100-μm coronal sections were cut, counterstained with bisbenzamide, and single or double exposure photomicrographs were taken by using fluorescence microscopy. Asterisk at B gives an example of the DiI crystal placement site. The double exposure shows both bisbenzamide-stained cells and DiI-labeled axons. **A:** In $Emx2^{+/+}$ brain at E15.5, labeled fibers reach the primitive internal capsule (arrow in A), beneath the ganglionic eminences (GE). **B–D:** At the same age in the $Emx2^{-/-}$ brain, the bundle of axons descending from the dorsal thalamus (DT) is misrouted in the ventral telencephalon after crossing the diencephalic–telencephalic boundary (double arrowheads in B and C). The normal component of the thalamic fibers traveling toward the cortex can be followed in adjacent rostral sections (arrows in C and D). **E,F:** High-power views of thalamic fibers reaching the cortex (Ctx) at E15.5 in the normal and mutant *Emx2* brains, respectively. In the $Emx2^{-/-}$, fewer fibers enter the cortical intermediate zone. **G,H:** High-power views of the thalamic axons shown at C and D. **I,J:** DiI-labeled thalamic projections in E18.5 WT (I) and $Emx2^{-/-}$ (J) brains, demonstrating the misrouted fibers in the ventral telencephalon (double arrowhead in J). **K,L:** Adjacent sections to J (anterior and posterior, respectively) in the $Emx2^{-/-}$ mouse brain, demonstrating the course of the two labeled fiber bundles. K contains normal (arrow), whereas L contains mostly abnormal thalamic projections traveling ventrally (double arrowhead). **M,N:** Higher magnification of thalamic axons approaching the cortex at the corticostriatal junction in WT (M) and $Emx2^{-/-}$ brain (N). In the mutant, there are relatively fewer fibers and the fasciculation pattern is altered (double arrowhead in N). **O,P:** High-power images of K and L. LV, lateral ventricle. Scale bars = 200 μm in A (applies to A–D), 50 μm in E (applies to E,F), 50 μm in O (applies to O,P), 100 μm in G (applies to G,H), 100 μm in I (applies to I–L), 100 μm in M (applies to M,N).

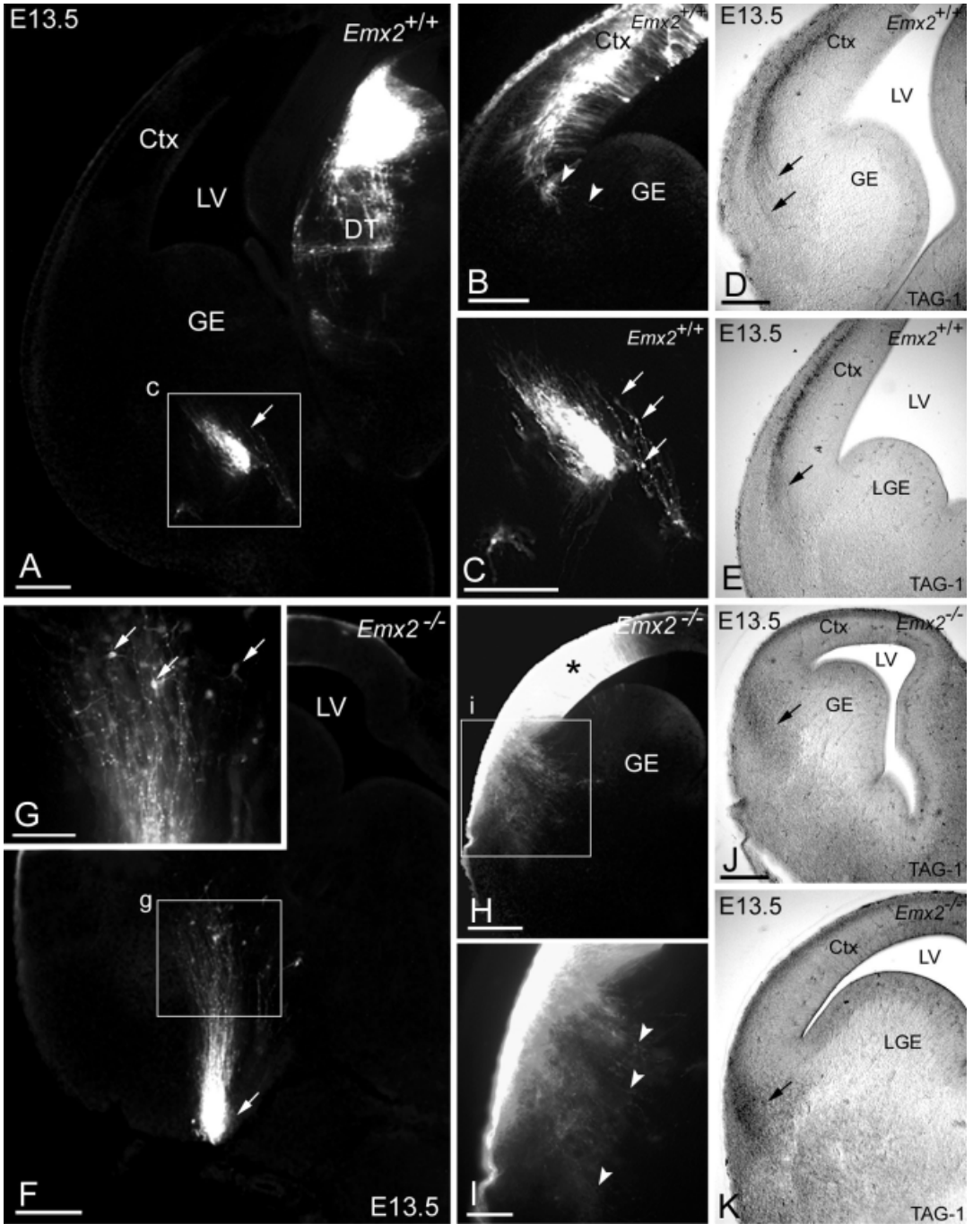

Figure 3

ever, at later ages (E17.5 and 18.5), when the projections have crossed the striatocortical junction, no differences were apparent at the same segment of the corticofugal axons between WT and mutant *Emx2* mice (Fig. 6A–D; also see Fig. 8E–H). In both cases, the labeled corticofugal axons crossed the anlage of the striatum in similarly patterned fascicules. By this stage, cortical crystal placements revealed both thalamocortical and corticofugal projections and it is conceivable that the misplaced fiber bundles at the striatocortical junction contained aberrant corticofugal projections (see Fig. 7C–E). The interhemispheric axons were observed entering the corpus callosum from anterior cortical crystal placement sites (Fig. 6A,B).

Topographic studies. After E16.5, placement of several crystals of different carbocyanine dyes (alternating DiI, DiA, DiI) into the cortex (see schematic drawing of Fig. 6) labeled bundles of closely mixed corticofugal and thalamocortical axons (Molnár et al., 1998a). From serial confocal microscopic optical sections, high-resolution reconstructions were prepared to reveal the fine topography of stained fibers within the entire bundle between the thalamus and the cortex. From a single crystal placement in the $Emx2^{+/+}$ cortex, the backlabeled thalamic cells tend to form an anteroposteriorly elongated segment when observed in horizontal sections (Fig. 6E). Different crystals placed in a parasagittal line along the hemisphere in an $Emx2^{+/+}$ brain at E16.5 revealed that more anterior cortical regions are innervated by more medial segments within the developing thalamus, whereas more posterior cortical regions receive projections from more lateral thalamic segments (Fig. 6E). However, in the $Emx2^{-/-}$ brains, the topography of the backlabeled cells in the thalamus is not completely conserved. The groups of thalamic cells backlabeled from similar regions of the dorsal cortex appear to have shifted to more medial and anterior locations (Fig. 6F,G) compared with normal (Fig. 6E). Our observations on the topography of these projections confirmed the previous findings of Mallamaci et al. (2000b) and Bishop et al. (2000), who described a shift in the areal identity in $Emx2^{-/-}$ brains. These authors found that, in this mutant, the caudal–medial cortical areas are reduced in size and the anterior–lateral cortical areas are expanded in size. However, in the $Emx2^{-/-}$ brains, the overall relative topography of the backlabeled cells in the thalamus from cortical crystal placements is conserved, and the interlinking fiber bundles extend separately and in an orderly manner while crossing the internal capsule.

Cortical carbocyanine crystal placement revealed the aberrant path of thalamocortical connectivity. To investigate whether the derailed thalamic axons reach the dorsal cortex, we placed carbocyanine dyes into different cortical areas at E18.5, similar to that shown in Figure 6. Coronal sectioning allowed us to follow the path of the labeled fiber bundles containing thalamocortical and corticofugal projections. We observed that a large number of fibers from different cortical areas took an aberrant route, descended to the ventral margin of the telencephalon–diencephalon junction in $Emx2^{-/-}$ brains (compare Fig. 7E with N). Because these bundles contained both thalamocortical and corticofugal projections, both sets were affected by the abnormality. Different cortical carbocyanine crystal placements revealed distinct groups of backlabeled thalamic cells (Fig. 7J,K,L). This demonstrates that the derailed thalamic fibers finally reach the cortex through these aberrant routes. In addition to the defect in thalamic connectivity, we also observed reduction in labeled fibers in the cerebral peduncles on caudal sections (compare Fig. 7M and R). These results may suggest that corticofugal projections normally destined for the cerebral peduncle terminate at the ventral surface in the aberrant fiber bundle, a finding that shows similarity to the *Nkx2-1*-deficient phenotype (Marín et al., 2002). However, in the *Nkx2-1* mutant mouse, the thalamocortical connectivity appears normal.

Double labeling from cortex and thalamus. To examine the relationship between the thalamic and corticofugal projections, synchronous tracing from cortex and thalamus at E15.5 and E17.5 was used. A single DiI crystal was placed into the dorsal thalamus (putative ventrobasal complex or lateral geniculate nucleus [LGN]) to

Fig. 3. 1,1′-Dioctadecyl-3,3,3′,3′-tetramethylindocarbocyanine perchlorate (DiI) placement into the dorsal thalamus at embryonic day (E) 13.5 revealed that the trajectories of the early thalamocortical and internal capsule cell projections are both drastically altered in the *Emx2* knockout (KO) mice. The early corticofugal projections, revealed with dorsal cortical placements of DiI, were also abnormal. This finding was confirmed using immunohistochemistry for TAG-1. Fixed E13.5 brains received two DiI placements: one into the dorsal thalamus (DT) of one hemisphere and the other into the contralateral dorsal cortex. **A:** Demonstration of the entry of labeled early thalamocortical projections to the telencephalon in the WT brain. Dorsal thalamic crystal placements also revealed backlabeled cells in the ventral thalamus and in the primitive internal capsule (arrow at A). **C:** High-power image from the region contained within the box at A. Arrows show examples for backlabeled cell bodies. **B:** Example of labeling pattern observed from a cortical DiI crystal placement in wild-type (WT) brain at E13.5. The corticofugal fibers extend ventrally below the primitive cortical plate through the intermediate zone and turn toward the ganglionic eminence (GE, arrowheads). **D,E:** Demonstrate the distribution of TAG-1 immunoreactivity in two sections taken from levels similar to that shown in B. Both sections are from the same E13.5 WT brain. TAG-1, a marker of corticofugal fibers, is expressed in the cortical intermediate zone and can be followed in fibers toward the striatocortical junction (arrows) along trajectories similar to those observed with DiI tracing (B). **F,G:** In *Emx2* KO brains, dorsal thalamic crystal placement labeled early thalamic axons anterogradely and internal capsule cells retrogradely. There was a striking difference between the trajectories observed in WT and KO. In the *Emx2* KO brain, the labeled fiber bundle descended to the ventral margin of the diencephalon–telencephalon boundary (arrow at F) and then ascended to the internal capsule, where numerous backlabeled cells were observed. G: High-power image taken from the region indicated with a box at F. Arrows at G depict examples of labeled cell bodies. In WT, the labeled bundle traversed the same boundary at the midpoint (compare the location of the arrow at A and F). **H,I:** DiI crystal placement in the dorsal cortex (asterisk) revealed numerous corticofugal axons descending to the striatocortical junction in the *Emx2* KO brain at E13.5. They appeared to extend along a more superficial path, closer to the pial surface, and not below the forming cortical plate as observed in WT (compare B and H). I: High-power picture taken from the region indicated with a box at H, demonstrating that the labeled fiber bundle fans out more widely in the *Emx2* KO than in WT (arrowheads). **J,K:** Distribution of TAG-1 immunoreactivity on two different coronal sections from an E13.5 *Emx2* KO brain. TAG-1 immunoreactivity was located closer to the pial surface and matched the displaced location of corticofugal projections observed with DiI tracing (compare H and K). Despite this abnormality, the front of the TAG-1 immunoreactivity (and the corticofugal projections) extended to similar regions of the striatocortical junction (arrows at D,E,J,K). LGE, lateral ganglionic eminence; LV, lateral ventricle; Ctx, cortex. Scale bars = 200 μm in A–F,H,J,K, 100 μm in G,I.

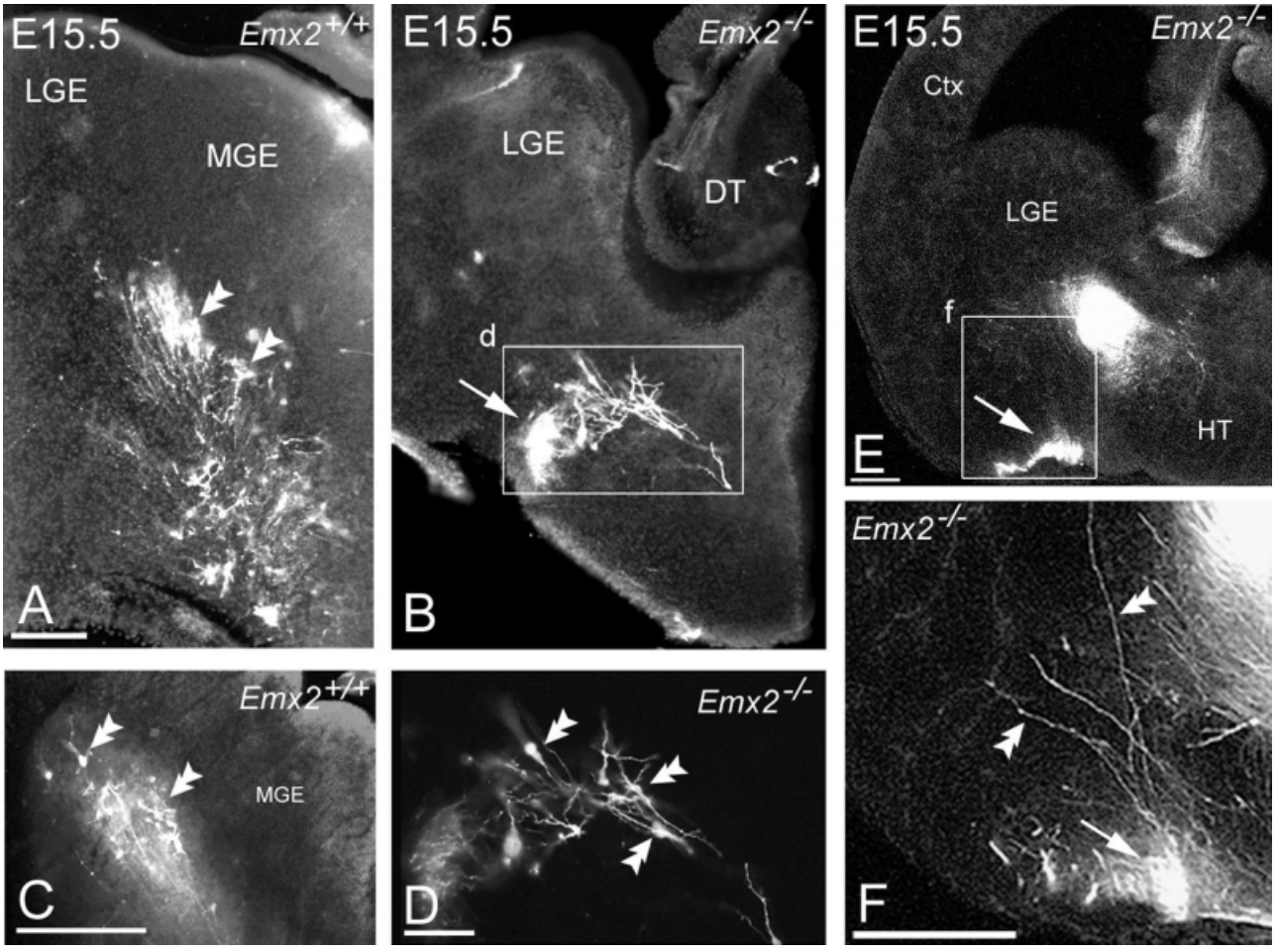

Fig. 4. 1,1′-Dioctadecyl-3,3,3′,3′-tetramethylindocarbocyanine perchlorate (DiI) crystal placements into dorsal thalamus revealed that the backlabeled cells in the primitive internal capsule are displaced in *Emx2*$^{-/-}$ mice. A small crystal of DiI was implanted into the dorsal lateral part of the dorsal thalamus of the left hemisphere of fixed embryonic day (E) 15.5 *Emx2* wild-type (WT) and mutant mice brains. **A,C:** After dorsal thalamic DiI placements, numerous cells were backlabeled in the internal capsule, below the medial and lateral ganglionic eminences (MGE and LGE, respectively) in normal *Emx2* mice (double arrowheads). **B,D:** Displaced location of the backlabeled cells under the primitive internal capsule in the *Emx2*$^{-/-}$ mice (double arrowheads in D). In all the cases studied, backlabeled cells in the mutant were located more ventrally in the telencephalon, close to ventral telencephalic areas. This area corresponded to the displaced thalamic axons (arrow in B). **E:** Coronal section of an *Emx2*$^{-/-}$ E15.5 telencephalon, showing the ventral telencephalic misrouted DiI-labeled fibers (arrow) after dorsal thalamic DiI crystal placement. **F:** High-power view of the region indicated with white box in E. Note the presence of some ascending compensating thalamic projections (double arrowheads) growing toward the internal capsule from the misrouted bundle at the ventral telencephalic–diencephalic boundary (arrow). Scale bars = 100 μm in A (applies to A,B), 100 μm in C, 50 μm in D,F, 200 μm in E.

reveal the ascending thalamic fibers together with a single DiA crystal into the dorsal cortex (putative somatosensory or visual areas) to reveal the descending corticofugal projections within the same hemisphere. Incubation periods that optimized both the anterograde and retrograde labeling (4 weeks at room temperature at E15.5) were used. At E15.5, the labeled thalamic and early corticofugal projections formed common fascicules within the lateral part of the internal capsule. The two fiber systems showed intimate association in both *Emx2*$^{+/+}$ and *Emx2*$^{+/-}$ brains (Fig. 8A,B and C,D). In *Emx2*$^{-/-}$ brains, the two sets of fibers also met at the same region of the lateral part of the internal capsule, but the corticofugal projections that deviated laterally and ventrally did not mingle with the thalamic fibers, and thalamic projections were less numerous (Fig. 8C,D). At E17.5 in WT brains, corticofugal projections reached the dorsal thalamus and both sets of fibers intermingled at the internal capsule (Fig. 8E,F). In the *Emx2*$^{-/-}$, similar results were found, i.e., corticofugal axons reached the thalamus and thalamic fibers also entered in the cortex extending in the intermediate and subplate zones. However, less thalamic fibers were observed reaching the cortex (Fig. 8G,H).

Immunohistochemistry

L1. The overall distribution of thalamocortical connections in *Emx2*$^{-/-}$ brains was also examined by using a polyclonal antibody against L1. L1 is a cell-adhesion molecule, thought to be specifically expressed on thalamocortical and other diencephalic axons (Godfraind et al., 1988; Fukuda et al., 1997). Immunohistochemistry for L1 in *Emx2*$^{-/-}$ brains at E15.5 revealed a conspicuous axon

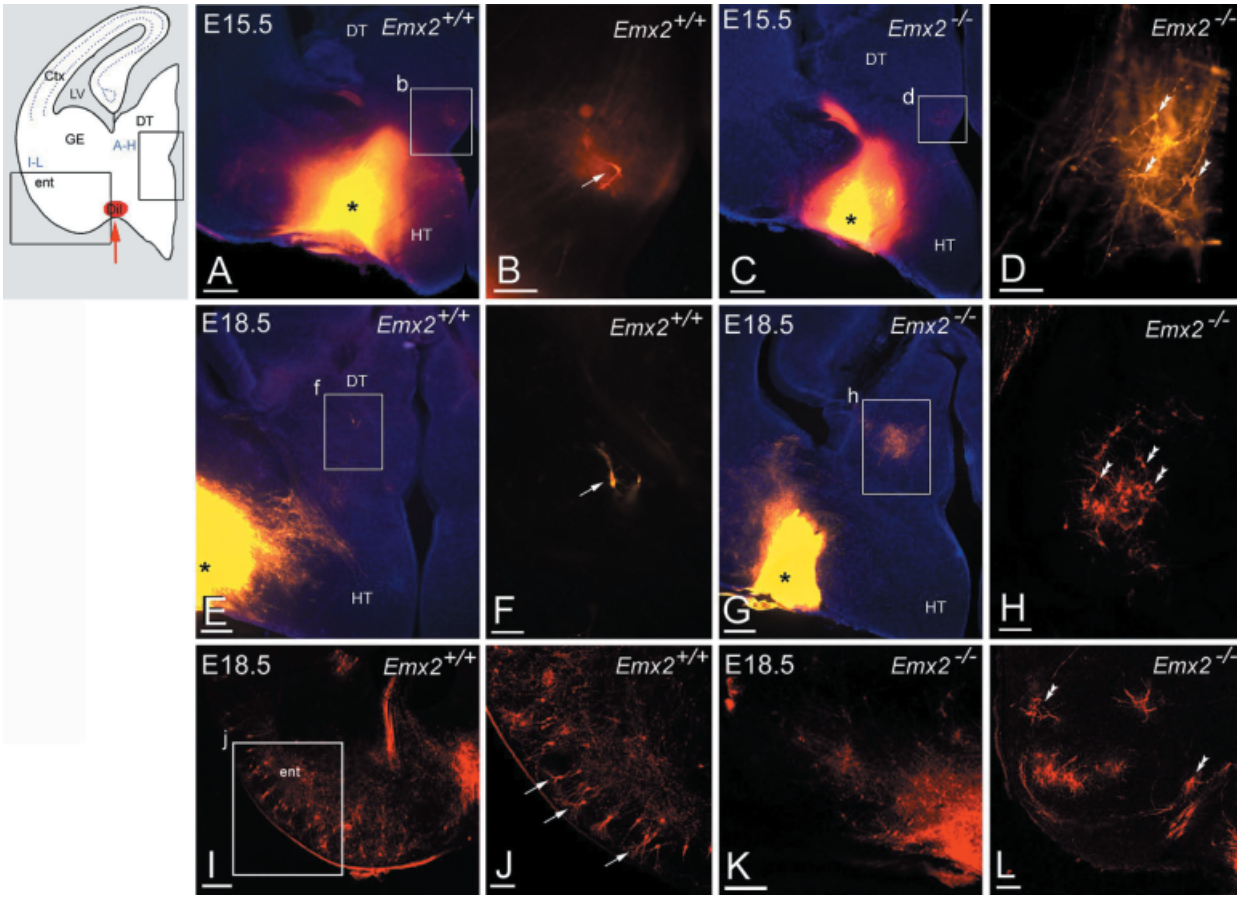

Fig. 5. 1,1′-Dioctadecyl-3,3,3′,3′-tetramethylindocarbocyanine perchlorate (DiI) crystal placement to the ventral telencephalon at the telencephalon–diencephalon boundary revealed the source of the aberrant thalamofugal axons and demonstrated the altered entorhinal cortical projections. A small crystal of DiI was implanted into the ventromedial part of the telencephalon of embryonic day (E) 15.5 and E18.5 *Emx2* wild-type (WT) and mutant mice brains. The schematic panel depicts the site of DiI placement (red arrow) and the regions of the section where the photomicrographs were taken (boxes). Asterisks at A, C, E, and G indicate the DiI crystal placement sites. B is higher magnification image of A, D of C, F of E, and H of G. **A–D:** At E15.5, more numerous cells were backlabeled in the $Emx2^{-/-}$ dorsomedial thalamus (double arrowheads in D) than in the $Emx2^{+/+}$ (arrow in B). **E–H:** At E18.5, more backlabeled cells were found in the dorsal thalamus of the $Emx2^{-/-}$ brain (H) than in the WT (F). The difference between the WT (E,F) and mutant (G,H) at E18.5 was even more apparent than in the earlier ages. Note the location and morphology of the labeled dorsal thalamic cells in the mutant (double arrowheads in H). After DiI placement into the ventral part of the telencephalic–diencephalic junction at E18.5, the distribution and somatodendritic morphology of backlabeled cells in the entorhinal cortex of $Emx2^{+/+}$ (I,J) and $Emx2^{-/-}$ (K,L) brains appeared different. In the WT, the labeled entorhinal cells line up in an organized manner (arrows at J), whereas in the mutant, their position and orientation appear random (double arrowheads at L). DT, dorsal thalamus ; HT, hypothalamus ; ent, entorhinal cortex ; Ctx, cerebral cortex ; GE, ganglionic eminences. Scale bars = 200 μm in A,C,E,G, 100 μm in B,D,F,H,I,K, 50 μm in J,L.

bundle connecting the dorsal thalamus and the basal-marginal telencephalon (Fig. 9B). This bundle was not detected in WT brains (Fig. 9A). Interestingly, in the $Emx2^{-/-}$ brains, only a few of the L1-immunoreactive fibers reached the cortex (Fig. 9D) compared with $Emx2^{+/+}$ brains (Fig. 9C). This observation suggests that either there was a delay in $Emx2^{-/-}$ thalamic fibers reaching the cortex or that a large fraction of the thalamic fibers were misrouted at the telencephalic-diencephalic border.

At E17.5, L1-positive thalamic fibers reached the cortex in both $Emx2^{+/+}$ and $Emx2^{-/-}$ brains (Fig. 10A,B,E,F). On the other hand, L1-positive fibers exhibited a different pattern of fasciculation in the internal capsule of the $Emx2^{-/-}$ mice (compare Fig. 10C with D). At the thalamic level, L1-positive fibers were misrouted toward the ventral diencephalon (Fig. 10D). These misrouted fibers were not detected in WT brains, but rather all L1-immunoreactive thalamic fibers turned at the telencephalic–diencephalic border to enter the internal capsule (Fig. 10C). The distinct changes in the fasciculation pattern were not as striking at the striatocortical junction in the mutant.

TAG-1. The trajectory of corticofugal fibers in mutant brains was examined by using the mouse monoclonal TAG-1 4D7 antibody (Yamamoto et al., 1986), which was shown to be a specific marker of early corticofugal projections (Denaxa et al., 2001). Tracing with carbocyanine dyes in $Emx2^{-/-}$ animals indicated that corticofugal projections initially extend more superficially at E13.5 (Fig. 3J,K) and a small number of early corticofugal axons project to abnormal positions in the basal telencephalon (Fig. 8C). Alterations in the immunohistochemical localization of TAG-1 in the brains of E13.5 mutant animals

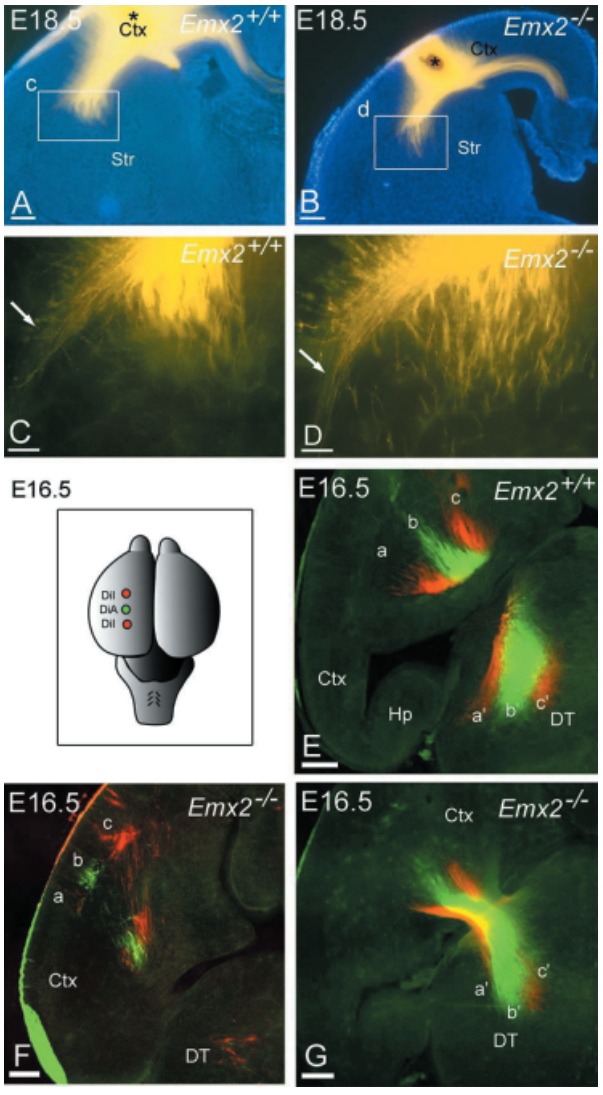

Fig. 6. Tracing from the dorsal cortex revealed at embryonic day (E) 16.5 (E–G) and E18.5 (A–D) corticofugal, callosal, and thalamic projections and their topography in wild-type (WT) and mutant *Emx2* mice. **A,C:** 4-(4-(dihexadecylamino) styryl)-*N*-methylpyridinium iodide (DiA) crystal placement site (asterisk at A) in the cortex (Ctx), demonstrating the normal fasciculation pattern through the anlage of the striatum (Str) in a WT E18.5 brain. **B,D:** A similar normal projection pattern in an E18.5 $Emx2^{-/-}$ brain. Note that the corpus callosum is present in the mutant. C is a higher magnification image of the area labeled with the box in A and D of the area boxed at B. **E:** Multiple carbocyanine crystal placements along an anterior–posterior line in the cortex (schematic panel) revealed the topographic order of projections and the backlabeled thalamic cells in an E16.5 WT mouse. Brains were sectioned in the horizontal plane. Crystal placements at a,b,c labeled thalamic cell groups at a′, b′, c′ respectively. **F,G:** High-power view of the labeled projections and backlabeled cell groups in the dorsal thalamus of an E16.5 $Emx2^{-/-}$ brain from similar carbocyanine crystal placement sites. Notice the medial and anterior shift of the labeled cells in the mutant (a′,b′,c′ at G) compared with WT (a′,b′,c′ at E). DT, dorsal thalamus; Hp, hippocampus; LV, lateral ventricle. Scale bars = 100 μm in A,B,E–G, 50 μm in C,D.

was detected, which confirmed the findings obtained with DiI tracing. Unfortunately, TAG-1 immunohistochemistry is not clearly detectable on the corticofugal projections for their entire length; the strength of reactivity reduces substantially after the striatocortical junction. TAG-1 immunohistochemical staining of $Emx2^{-/-}$ animals at E15.5 and E17.5 brains revealed a normal pattern of expression, with no apparent changes in the trajectory of the corticofugal fibers (Fig. 11D,H) but could not reveal the subsequent path of the corticofugal projections. Alternative methods are needed to examine the corticofugal and thalamocortical components of the aberrant bundles described at Figure 7 in the $Emx2^{-/-}$ brains. In the $Emx2^{+/+}$, $Emx2^{+/-}$, and $Emx2^{-/-}$ brains, TAG-1–immunopositive, radially oriented fibers were observed in the marginal zone, cortical plate, subplate, and IZ (Fig. 11E,F,K,L). The only difference that we observed in $Emx2^{-/-}$ brains was that the immunoreactivity in the marginal zone and cortical plate was significantly reduced (compare Fig. 11E,F with K,L, respectively).

DISCUSSION

This study revealed that, in $Emx2^{-/-}$ brains, a large number of early thalamic projections reach the cortex through an aberrant route. Thalamic axons descend from the dorsal thalamus but enter the telencephalon abnormally, at the ventral-most point of the diencephalon–telencephalon junction. However, a subset of thalamic axons entered the internal capsule normally and continued to grow through the striatal anlage toward the cerebral cortex in $Emx2^{-/-}$ brains. At E15.5, corticofugal projections descended into the internal capsule where they intermingled with the thalamic axons. However, in the mutant brains, a small subset of the corticofugal projections deviated laterally and ventrally and did not mingle with thalamic fibers. Thalamic projections, that crossed the internal capsule were overall less numerous at this stage in the mutant. By E17.5, these projections reached all parts of the cortex; however, in $Emx2^{-/-}$ brains, fewer fibers accumulated below the cortical plate. These observations, which were supported by the L1 and TAG-1 expression results, led us to the conclusion that in $Emx2^{-/-}$ brains a large proportion of the thalamocortical projections have an altered and delayed arrival to the cortex. These alterations may contribute to the shift in cortical areal identity.

Altered distribution embryonic internal capsule cells and their early thalamic projections in $Emx2^{-/-}$ mouse

Previous tracing experiments have revealed the order that thalamic fibers maintain, and the cellular elements that they encounter while growing out from the diencephalon, through the internal capsule, and accumulating below the corresponding cortical region (McConnell et al., 1989; Catalano et al., 1991, 1996; Allendoerfer and Shatz, 1994; Molnár, 1998). Thalamic afferents reach the cortex by associating with preexisting cells and their early projections in the ventral thalamus, internal capsule, and preplate (De Carlos and O'Leary, 1992; Erzurumlu and Jhaveri, 1992; Métin and Godement, 1996; Molnár et al., 1998a,b,c). The guiding role of these premature networks of connections was thought to be important for the thalamic fibers to find their way to the cortex through the subdivisions of the embryonic forebrain. In addition, gradients of molecular cues might be present in the cortex, which aid in these guiding processes. Connectional analysis in mammalian embryonic brains revealed that tha-

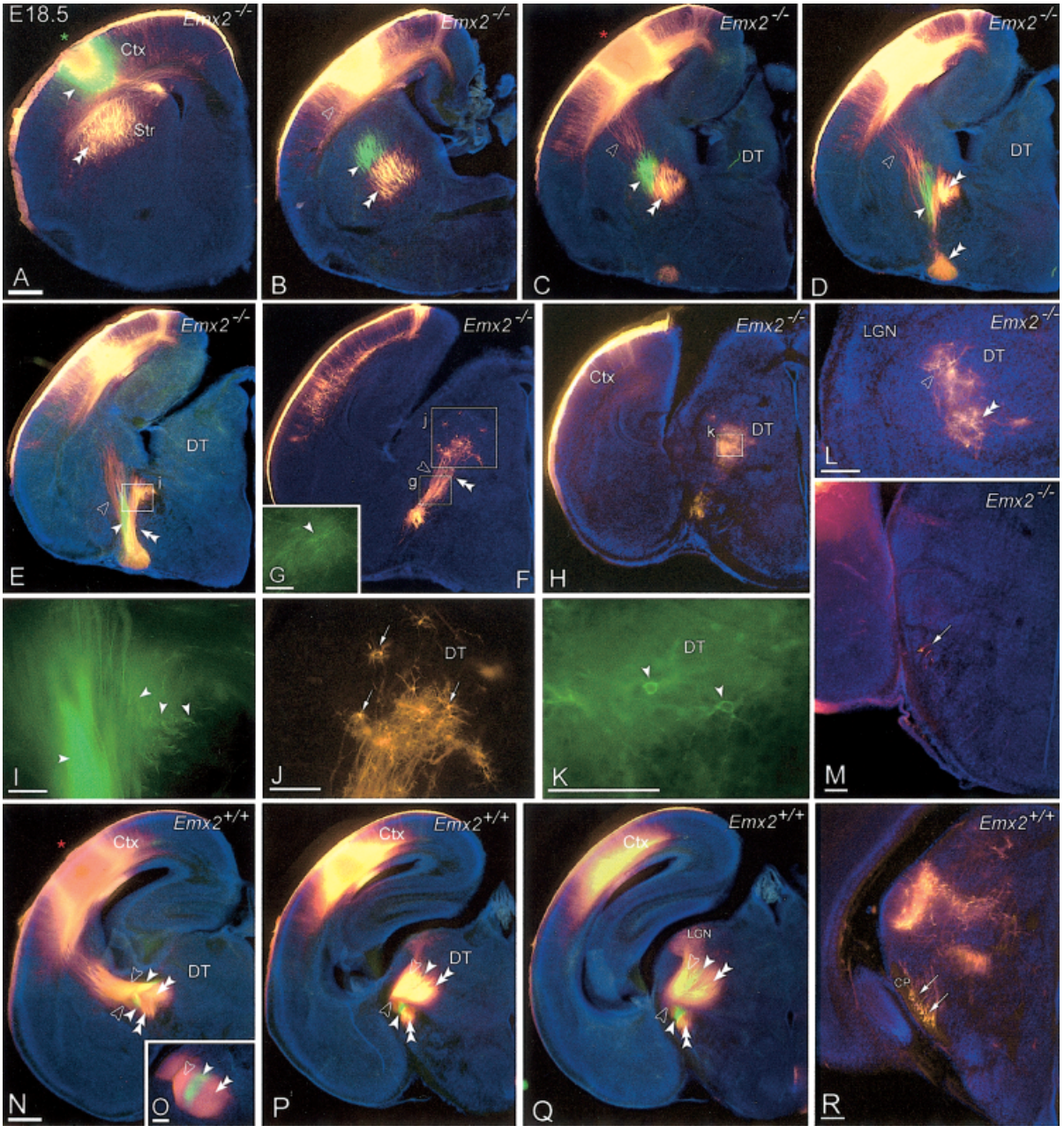

Fig. 7. At embryonic day (E) 18.5 multiple carbocyanine crystals were placed along an anterior–posterior line in the cortex (Ctx; as demonstrated in the schematic drawing of Fig. 6). The labeled corticofugal and thalamic projections were examined in wild-type (WT; *Emx2*$^{+/+}$, N–R) and in mutant mice (*Emx2*$^{-/-}$, A–M). **A–H:** Serial coronal sections (100 μm) revealed the path and topography of projections from three separate crystal placement sites. Double arrowheads depict the fiber bundles labeled from the anterior cortical 1,1′-dioctadecyl-3,3,3′,3′-tetramethylindocarbocyanine perchlorate (DiI) crystal placement (appears red/orange), arrowheads label the fiber bundles labeled from the medial cortical 4-(4-(dihexadecylamino) styryl)-*N*-methylpyridinium iodide (DiA) crystal placement (appears green), and the open arrowheads indicate the bundles labeled from the posterior cortical DiI crystal placement (appears red/orange). It is evident that some of the labeled fibers descend to the ventral part of the diencephalon–telencephalon junction and then can be followed to backlabeled groups of thalamic cells (see F and J). **I:** High-power picture taken from the region indicated with the box at E to show the pattern of labeled fibers in the middle (green) bundle (filled arrowheads at E and I), because they are not apparent with low power. G: High-power image, taken with using only green filter, from the region indicated with a box labeled g in F to show evidence that fibers from the green bundle were also ascending to a labeled dorsal thalamic cell group (see K). **J:** High-power picture taken from the backlabeled group of thalamic cells labeled in F. **L:** The rostral and caudal DiI placements labeled two separate cell groups (double arrowhead and open arrowhead in L, respectively). Note that both sets of backlabeled cells were seen in the ventrobasal part of the dorsal thalamus, whereas the dorsal lateral geniculate nucleus (LGN) does not contain labeled cells. This finding confirms the shift observed in the horizontal plane in Figure 6G in the coronal plane. **M:** In caudal sections, very few or no labeled fibers were observed in the cerebral peduncle in the mutant brain. **N–Q:** In WT, similar crystal placements labeled three separate fiber bundles, which travel though the internal capsule without descending to the ventral part of the diencephalic–telencephalic boundary (compare E with N). On arriving at that region, the fibers of the cerebral peduncle deviate ventrally from the thalamocortical connectivity (arrowheads pointing upward at N–Q depict the fibers descending toward the cerebral peduncle). Note that occipital crystal placement revealed labeled cells in LGN (Q). O: High-power view of the backlabeled cell groups in the dorsal thalamus of the adjacent section of the same E18.5 *Emx2*$^{+/+}$ brain. Notice the segregation of the labeled cells into three groups. **R:** In WT, on sections corresponding to the level of section shown at M from the mutant, numerous labeled fibers can be followed in the cerebral peduncle (CP). Scale bars = 400 μm in A (applies to A–F,H), in N (applies to N,P,Q), 200 μm in G,I,J,L,M,O,R, 100 μm in K.

lamic reticular cells (Mitrofanis and Guillery, 1993) and cells of the primitive internal capsule (Métin and Godement, 1996; Molnár et al., 1998a; Tuttle et al., 1999) project to the dorsal thalamus from early embryonic ages. There is a transient stripe of cells at the striatocortical junction; these cells have a characteristic gene expression pattern (*Map2*, *Calbindin*, *Pax6*) and lack thalamic connections. These cells, however, are distinct from the cells of the internal capsule with thalamic projections (Molnár, 2000). It is thought that the internal capsule cells with thalamic projections might be responsible for the early outgrowth of thalamic fibers and perhaps for the sorting of various corticofugal projections (Mitrofanis and Guillery, 1993). This idea is supported by the observations that, in *Mash1*$^{-/-}$ mice, thalamic projections did not enter the internal capsule when these cells were absent (Tuttle et al., 1999). In *Emx2*$^{-/-}$ mice, some of the backlabeled internal capsule cells and their projections were displaced ventrally and they appeared as a more dispersed cell group. The derailed early projections from thalamus followed the altered location of these internal capsule cells and their projections to the thalamus. It is possible that only a fraction of these internal capsule cells were displaced, which would affect only a subset of the thalamic projections. However, in *Emx2* mutants, the aberrant thalamic axonal bundle, pointing to the ventral-marginal telencephalon, could also have a distinct origin. EMX2-immunopositive cells are normally detected at the boundary between dorsal and ventral thalamus as well as in the marginal part of the basal-medial telencephalon (Fig. 1). The Emx2-immunopositive cells could provide repulsive clues for thalamic axons, thus directing them to turn toward the cortex. The absence of these cells (or their inappropriate differentiation and/or improper migration) in *Emx2* null mutants could account for the altered thalamocortical projections. There were more backlabeled cells in the ventromedial aspect of the dorsal thalamus in the *Emx2*$^{-/-}$ mouse compared with the WT in tracing experiments from the ventral part of the telencephalic-diencephalic junction. Therefore, it could be concluded that the ventromedial region of the dorsal thalamus is most severely affected by the lack of *Emx2* than any other projections from dorsal thalamus at early stages.

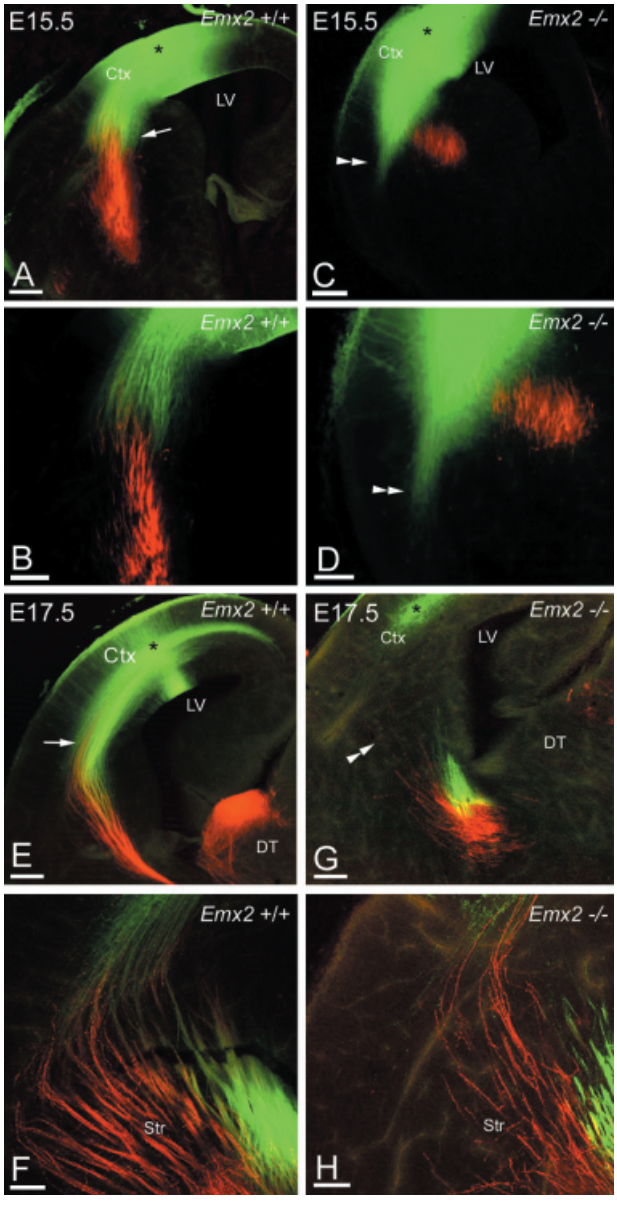

Fig. 8. Evidence demonstrating that thalamic and early corticofugal axons interact in the internal capsule in wild-type (WT) and mutant *Emx2*$^{-/-}$ mice at two different ages of embryonic development (A–D at embryonic day [E] 15.5 and E–H at E17.5). A,B,E,F are from WT; C,D,G,H are from *Emx2*$^{-/-}$ mice. Crystals of two different carbocyanine dyes, which could be distinguished from each other, were used to backlabel cells. A 1,1′-dioctadecyl-3,3,3′,3′-tetramethylindocarbocyanine perchlorate (DiI) crystal (orange-red) was placed in the dorsolateral thalamus (DT, into the lateral geniculate nucleus), and a 4-(4-(dihexadecylamino) styryl)-*N*-methylpyridinium iodide (DiA) crystal (green) was placed into the corresponding region of the occipital cortex (Ctx) of the same hemisphere (putative area 17, cortical crystal placement indicated with a black asterisk in A,C,E,G). To study the relationship between the developing thalamic projection and the earliest descending corticofugal axons, *Emx2*$^{+/+}$ (A,B,E,F) and *Emx2*$^{-/-}$ (C,D,G,H) brains were sectioned coronally through the primitive internal capsule. **A:** In a normal *Emx2* E15.5 brain, the DiA-labeled (*green*) preplate fibers and DiI-labeled (*orange-red*) thalamic axons appeared to align and to intermingle at the point indicated by the arrow. LV marks the lateral ventricle. **B:** High-power view of the region indicated by the arrow in A. **C:** At the same age in the *Emx2*$^{-/-}$ brains, some of the early corticofugal fibers (labeled with DiA appearing *green*) have extended ventrally through the intermediate zone and turned medially, under and through the developing corpus striatum following the normal developmental pattern. However, some corticofugal fibers did not turn medially, but rather extended laterally and ventrally (double arrowhead). **D:** Detailed view of the region indicated with double arrowhead in C. **E:** At E17.5 in the normal *Emx2* mice, the thalamic fibers entered in the intermediate zone (arrow) and remained in the subplate zone. The corticofugal fibers had crossed the internal capsule and had arrived at the dorsal thalamic region. **F:** High-power view of the region indicated by the arrow in E. Note the normal fasciculation pattern of thalamic axons in the striatum (Str). **G:** In the *Emx2*$^{-/-}$ mice, fewer thalamic axons reached the cortex and entered in the intermediate zone (double arrowhead) compared with the WT mice (E). **H:** High-magnification image taken from the region indicated by double arrowheads at G. It demonstrates the detail of the fasciculation pattern of thalamic axons in the striatal area of the mutant *Emx2* mice. Scale bars = 200 μm in A–E,G, 100 μm in F,H.

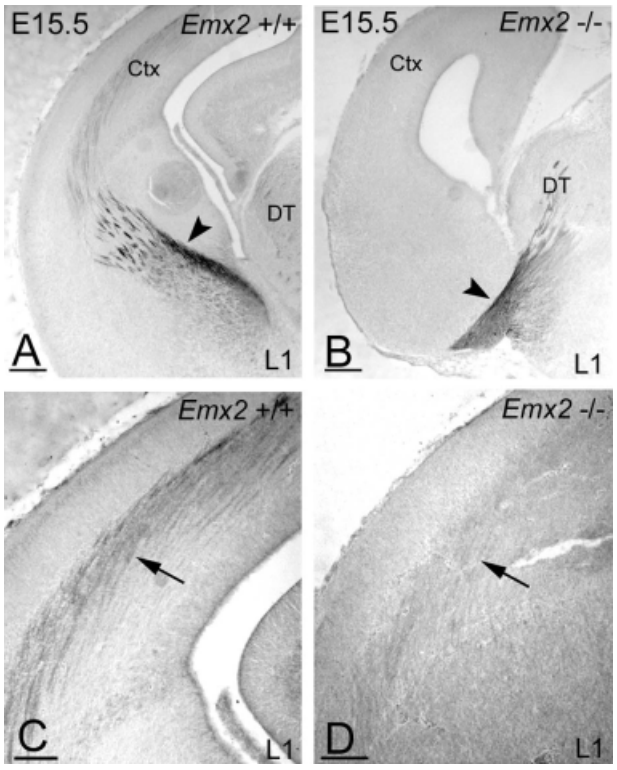

Fig. 9. Thalamic axons revealed with L1 immunohistochemistry in wild-type (WT; A,C) and *Emx2*$^{-/-}$ brains (B,D) at embryonic day (E) 15.5. **A,C:** L1-immunoreactive projections in WT extend from the dorsal thalamus (DT) through the internal capsule (arrowhead) toward the cortex (Ctx), where they terminate in the intermediate zone (arrow in C). C is a high-power view of the cortical region shown in A. **B,D:** In the *Emx2*$^{-/-}$ mice, L1 positive fibers extend from the diencephalon toward the ventral surface of the pallidum (arrowhead in B). In the intermediate zone of the *Emx2*$^{-/-}$ cortex (arrow in D), there was less intensive staining compared with WT. This finding might be due to the fewer thalamic fibers in the cortical intermediate zone in the *Emx2*$^{-/-}$ brains (arrow in D) compared with WT (arrow in C). D is a high-power view of the cortical region shown in B. Scale bars = 200 μm in A,B, 100 μm in C,D.

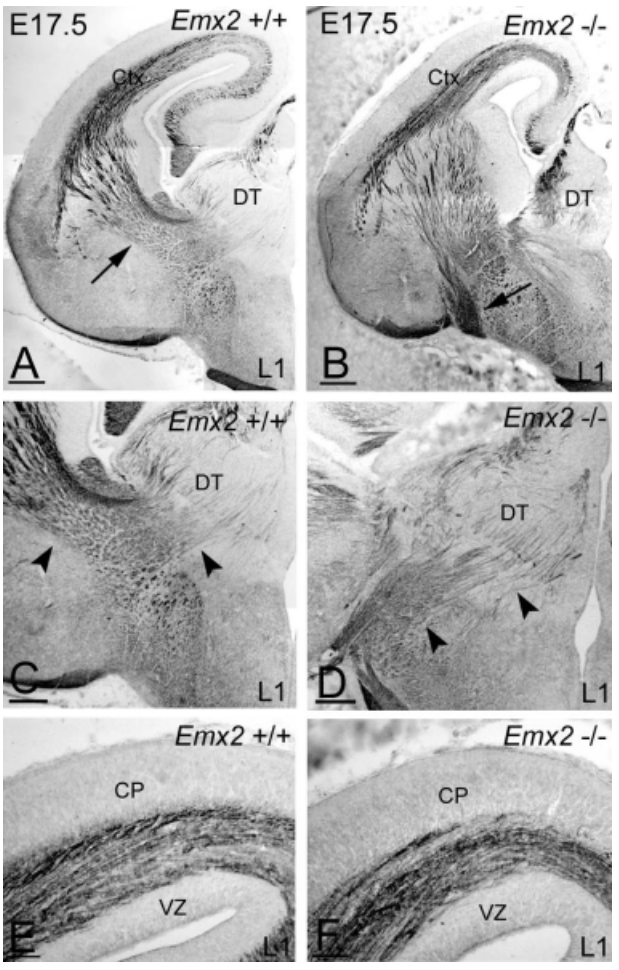

Fig. 10. L1 immunohistochemistry revealed thalamic and cortical connections at embryonic day (E) 17.5 in wild-type (WT; A,C,E) and *Emx2*$^{-/-}$ mice (B,D,F). **A:** Low-power view of the normal pattern of L1 immunoreactivity at E17.5. Most fibers travel within the internal capsule (arrow). **B:** In the *Emx2*$^{-/-}$ brains, a large number of axons deviate ventrally at the boundary between diencephalon and telencephalon (arrow). **C,D:** High-power photomicrographs of A and B (respectively). Note the axonal deviation demonstrated in the *Emx2*$^{-/-}$ brain (arrowheads D) compared with the WT (arrowheads in C). **E,F:** High-power photomicrographs of the dorsal cortex shown in A and B (respectively). By this age at E17.5, the L1 immunoreactivity appeared largely similar in both brains, demonstrating that a similar number of thalamic axons reach the cortex in *Emx2*$^{+/+}$ (E) and *Emx2*$^{-/-}$ (F), despite the differing routes of the axons. DT, dorsal thalamus; CP, cortical plate; VZ, ventricular zone; Ctx, cortex. Scale bars = 300 μm in A,B, 200 μm in C,D, 100 μm in E,F.

Altered early distribution of the entorhinal and perirhinal cortical connectivity in *Emx2*$^{-/-}$

The tracing experiments from the ventral part of the telencephalic–diencephalic junction showed an additional abnormality of the early connections. DiI crystal placement at the ventral part of the telencephalon–diencephalon junction, revealed that the distribution and morphology of numerous entorhinal and perirhinal cortical cells were different in the *Emx2*$^{-/-}$ compared with WT mice. The entorhinal cortex projects to the amygdala, and these projections might have been labeled from the crystal placements. It is also known that, from very early stages (E14 in rat), the ventral-most perirhinal cortical areas also send projections to the internal capsule (Molnár et al., 1998a). DiI crystal placement in the internal capsule backlabels cells located in the cortical plate of the perirhinal cortex. These early perirhinal cortical projections are among the first to extend through part of the internal capsule and may play a role in the guidance of thalamocortical fibers. It seems that the cells that give rise to the entorhinal and perirhinal cortical projections are also abnormally displaced in *Emx2*$^{-/-}$ mice. Rather than lining up in an organized manner, as in WT, these cells in the mutant appear randomly distributed in the ventral telencephalon. It seems, however, from our anterograde and retrograde tracing experiments and from L1 immunohistochemistry, that thalamic projections can compensate for the displacements of the internal capsule cells and the aberrant early projections. Although a large fraction of thalamic projection enters the telencephalon displaced more ventrally in *Emx2*$^{-/-}$ mice, most of them seem to find their way back toward the dorsal cortex (see Fig. 12). Nevertheless, the path, fasciculation pattern, and topog-

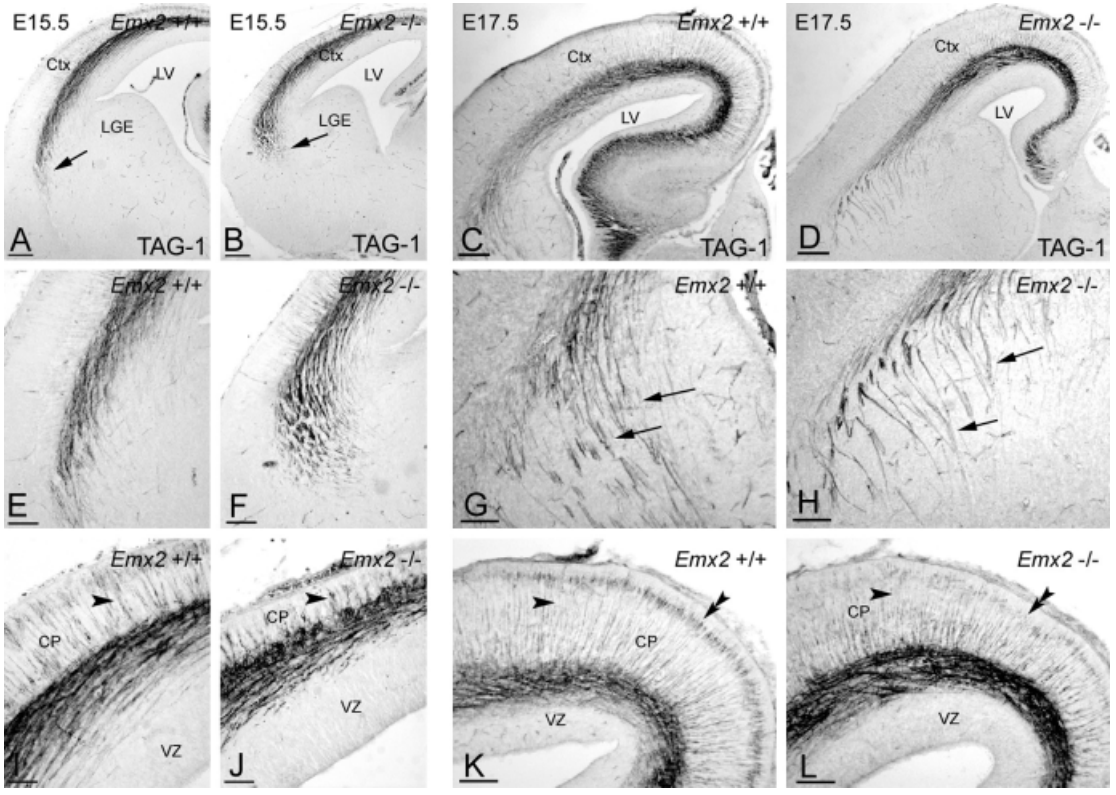

Fig. 11. TAG-1 immunoreactivity reveals minor abnormalities in the corticofugal connectivity in *Emx2*$^{-/-}$ brains at E15.5 and E17.5. The panels in the first column (A,E,I) are taken from wild-type (WT) and in the second column (B,F,J) from *Emx2*$^{-/-}$ mutants at embryonic day (E) 15.5. **A–D:** *Emx2*$^{+/+}$ (A,C) and *Emx2*$^{-/-}$ brains (B,D) show similar TAG-1–positive projections extending to the striatocortical junction (arrows). See G and H for high power. **I,J:** Demonstration of the altered pattern of the radially oriented TAG-1–positive fibers (arrowheads) in the cortical plate (CP) in the *Emx2*$^{-/-}$ brain. The panels in the third column (C,G,K) are taken from WT, and in the in fourth column (D,H,L) from *Emx2* mutants at E17.5. The pattern of TAG-1–positive projections extending into the striatum is similar in both the WT and the *Emx2*$^{-/-}$ brains. **G,H:** High-power photomicrographs from the striatocortical junction shown in C and D (respectively). Arrows depict examples of TAG-1–positive fiber bundles. **K,L:** High-power photomicrographs from the dorsal cortex in C and D (respectively). Note the reduced radial labeling (arrowhead in L) and reduced immunoreactivity in the superficial layers (double arrowheads in L) of the *Emx2*$^{-/-}$ (L) compared with the WT (K). Scale bars = 200 μm in A,B,G,H, 100 μm in C,D,I,J, 50 μm in E,F,K,L.

raphy of these redirected fibers are rather different from normal. Labeled axon bundles descending into the ventral telencephalon and diencephalon were observed with cortical crystal placement at E18.5 (Fig. 7E). These bundles contain retrogradely labeled thalamocortical and anterogradely labeled corticofugal projections. Identifying such bundles and the backlabeled group of thalamic cells has given compelling evidence that the subset of derailed thalamic fibers actually reach and enter into the dorsal cortex. Unfortunately, the marker TAG-1 is only expressed in the proximal segment of the corticofugal projections, which does not allow us to selectively label the entire corticofugal pathway.

Telencephalon–diencephalon junction is severely affected, but the corticostriatal junction is relatively intact in *Emx2*$^{-/-}$ mice

Hematoxylin-stained sections showed severe abnormalities in the telencephalon–diencephalon junction. The characteristic cell-free area of the internal capsule was displaced, and the intermediate zone of the developing cortex was not apparent in the mutant. It is known that growing axons change their growth kinetics and fasciculation patterns when they cross boundaries between two regions of distinct gene expression. The disturbed thalamocortical development in various transgenic mice mutants might be a very sensitive indicator of disturbed early forebrain regionalization and the consequences of altered choreography of development. From studies of various mutants, two common themes emerged. In one set of mutants (*Pax6*, *Tbr1*, *Gbx2*), thalamic projections arrested development at the lateral part of the internal capsule, close to the corticostriatal junction, whereas in other mutants (*Mash1*, *Sema6A*, and *Emx2*), the abnormality was at the telencephalon–diencephalon border (Hevner et al., 1998, 2001; Kawano et al., 1999; Tuttle et al., 1999; Leighton et al., 2001; present study). The telencephalon–diencephalon and corticostriatal junctions correspond to abrupt gene expression boundaries (Puelles et al., 2000).

***Corticostriatal junction in the Emx2*$^{-/-}$ mice.** The corticostriatal junction at the boundary of the developing mammalian pallium and pallidum appears to be critical for normal thalamocortical development. An interesting event involving thalamocortical and corticothalamic projections is observed at the lateral internal capsule close to the boundary slightly medial to the junction between cortical intermediate zone and the lateral ganglionic emi-

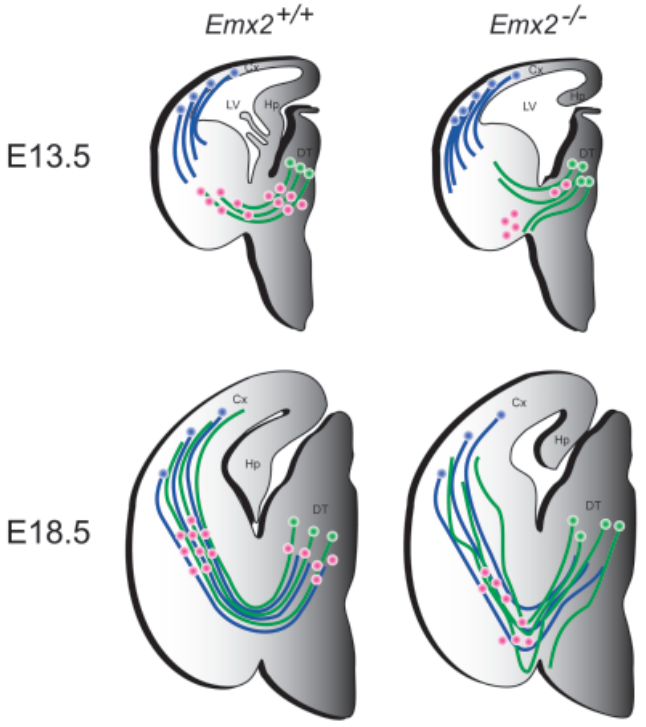

Fig. 12. Schematic summary of the establishment of early corticofugal and corticopetal projections in wild-type (WT; left column), and *Emx2*$^{-/-}$ mutant mice (right column). Each diagram represents a section through the left cerebral hemisphere, revealing the corticofugal (blue) and thalamocortical (green) pathways. *Pink* circles represent cells of the thalamic reticular nucleus and the primitive internal capsule, which possess dorsal thalamic projections. Green circles demonstrate cells of the dorsal thalamus, blue circles represent cells of preplate, the future marginal zone and subplate. At E13.5 (upper diagram), the preplate formation is not altered in the *Emx2* mutant compared with the WT animal. However, differences in the pathfinding of thalamic and corticofugal axons were seen between the two phenotypes. In the *Emx2*$^{-/-}$ brains, the corticofugal projections descended more superficially in the cortex and some did not turn medially at the corticostriatal junction but rather continued growing ventrally. A subset of thalamic axons reached the primitive internal capsule in the *Emx2*$^{-/-}$ mouse, the majority were misrouted in the ventral telencephalon as they crossed the telencephalic–diencephalic border. 1,1′-Dioctadecyl-3,3,3′,3′-tetramethylindocarbocyanine perchlorate (DiI) crystals placed in the dorsal thalamus of WT E14.5 animals backlabeled cells in the thalamic reticular nucleus, as described by Mitrofanis and Barker (1993), and within the primitive internal capsule (Métin and Godement, 1996). In mutant brains, backlabeled cells were distributed more ventrally in the internal capsule and their projections took an abnormal path, descending to the ventral edge of the diencephalic boundary. These aberrant axons were in close proximity to the misrouted thalamic fibers. By E18.5 (lower panels), the thalamocortical projections reached the appropriate cortical areas while associating with the early corticofugal fiber scaffold. Thalamic fibers establish a topographic map during the waiting period in the subplate. In the E18.5 *Emx2*$^{-/-}$ animals, fasciculation abnormalities occurred and some thalamic projections were misrouted at the telencephalon–diencephalon border similarly to earlier ages. At E18.5, the fascicles formed by thalamocortical axons in the striatum appear more disorganized, with fewer fibers reaching the cortex. As in earlier ages, backlabeled cells were seen in the thalamic reticular nucleus and in the medial internal capsule after DiI placement in the dorsal thalamus. In the mutant, some of these cells were displaced ventrally (pink circles). The displacement of these groups of cells in the thalamic reticular nucleus, internal capsule and other aberrant early connectivity in the region might also contribute to the delayed and altered arrival of the thalamic projections to the cortex. Cx, cortex; LV, lateral ventricle; Hp; hippocampus; DT, dorsal thalamus.

nence (Molnár and Hannan, 2000). During early stages of forebrain development, thalamocortical and corticofugal projections pause before they leave the primitive internal capsule and enter the cortex. After this brief pause in their extension, thalamic fibers cofasciculate with early corticofugal projections to reach the cortex (Molnár et al., 1998a). Liu and Graybiel (1992) and Métin and Godement (1996) described a narrow and dense stripe of calbindin- and MAP2-positive neurons at the lateral border of the lateral ganglionic eminence (LGE) in rat and hamster embryos. Stoykova and Gruss (1994) and Fernandez et al. (1998), described that *Pax6* expression terminates at this lateral border of the LGE, along a line that links the neuroepithelium of the striatocortical notch to the *Pax6*-positive neuron population of the basal telencephalon. Stoykova et al. (2000) have demonstrated recently that *Pax6* is also expressed in the ventricular zone (VZ) of the LGE; however, expression is at a much lower level than in the adjacent ventral pallidum. This pattern does not apply to *Emx2* expression. *Emx2* is expressed in the ventral pallidum but is not present in the ganglionic eminences (our unpublished results). The role of the stripe of cells expressing *Pax6* along the corticostriatal junction is not known; however, it seems to be critical for normal development of cortical connectivity. Hevner et al. (1998, 2001) and Kawano et al. (1999) described thalamocortical development in mice with transcription factor mutations expressed in either cortex (*Tbr1*), dorsal thalamus (*Gbx2*), or both (*Pax6*). They showed that these mutations caused aberration in corticothalamic and thalamocortical pathfinding in the region of the primitive internal capsule. It is not yet understood what events are responsible for these abnormalities at the corticostriatal junction (Molnár and Butler, 2002).

***Telencephalon–diencephalon junction in Emx2*$^{-/-}$ mice.** In *Emx2*$^{-/-}$ brains, thalamocortical projection abnormalities at the telencephalon–diencephalon boundary are most prominent. In these brains, there are very few misrouted corticofugal projections at the corticostriatal junction. The thalamocortical fiber misrouting at the telencephalon–diencephalon boundary is most probably independent of the early corticofugal connectivity, because it occurs at an earlier stage and at a location different from the interaction near the corticostriatal junction. This finding suggests that other factors may be responsible. The *Sema6A* mutant mice phenotype looks very similar to the *Emx2*$^{-/-}$ mutant mice (Leighton et al., 2001). In the Sema6A mutant, some of the thalamic projections also surface at the telencephalon–diencephalon boundary. The Sema6A expression in *Emx2*$^{-/-}$ mice is not known, but it could be a potential candidate molecule responsible for thalamocortical abnormality.

The medial thalamic regions project to the superficial layers of the limbic cortex, whereas the dorsolateral thalamic nuclei connect to the dorsal cortex (Krettek and Price, 1977; Robertson and Kaitz, 1981). The limbic system–associated membrane protein (LAMP) is known to be selectively expressed in the limbic cortex (Levitt, 1984). It was demonstrated that membranes containing LAMP promote axonal growth from the medial thalamus compared with growth from the dorsolateral thalamus (Mann et al., 1998). It appears that ephrin-A is expressed in the dorsal cortex, whereas ephrin-B3 is localized in limbic structures (Takemoto et al., 2001). Ephrin-A5, a ligand of EphA receptors, was shown to be expressed in the neocortex and to inhibit axonal growth from the medial thala-

mus without affecting dorsolateral thalamic axons (Gao et al., 1998). Takemoto et al. (2001) have provided evidence recently that ephrin-B3 was expressed to a greater extent in the limbic region and that it inhibited axonal growth in vitro from the lateral thalamus but not from the medial thalamus. Thus, ephrin-B3 could provide inhibitory influence on the lateral but not the medial thalamic projections. Sema6A, LAMP, ephrin-A5, ephrin-B3 might all cooperate in guiding the thalamic projections from the medial and lateral thalamic nuclei to the correct target areas of the limbic system and to the dorsal cortex. The expression of these molecules in *Emx2*$^{-/-}$ mutants needs to be studied further.

What is the origin of the altered thalamocortical projections in *Emx2*$^{-/-}$ mice?

Mallamaci et al. (2000b) and Bishop et al. (2000) described that there was a shift in the area identity in the cerebral cortex of *Emx2* mutant mice, which correlated with the altered distribution of thalamocortical projections. The most spectacular difference was shown with carbocyanine dye tracing from the occipital cortex. In WT brains, neurons of the LGN in the dorsal thalamus were backlabeled, whereas presumptive ventral-basal complex cells were backlabeled in *Emx2*$^{-/-}$ brains. In this study, DiI tracing from the LGN demonstrated that, although the thalamocortical fasciculation pattern was altered, some projections crossed the internal capsule and reached the proximity of the cortex. Also, the tracing experiments from the telencephalon-diencephalon junction showed that early projections from the ventromedial aspect of the thalamus were more severely affected than any other part of the dorsal thalamus at early stages. It appears that most of these misrouted thalamocortical projections recovered and ascended from the ventral telencephalon toward different cortical regions. The misrouting caused a considerable delay in thalamic fibers arriving to the cortex, which might contribute to the altered cortical topography. This study supports that the altered cortical topography is not exclusively due to the altered gene expression pattern on the cortical sheet, and earlier events, like axon elongation through the telencephalo-diencephalic junction and in the internal capsule, might also contribute to the described abnormalities.

In conclusion, a significant fraction of thalamic projections in *Emx2*$^{-/-}$ mice is misrouted at the telencephalon–diencephalon boundary, and this abnormality is associated with displaced projections of internal capsule cells and disrupted entorhinal and perirhinal cortical projections. Although this early targeting abnormality is linked with the altered *Emx2* expression pattern in the dorsal cortex and with aberrant growth of a fraction of the early corticofugal projections at the striatocortical junction, it most probably occurs independently from these events. The abnormalities are likely related to earlier guidance defects, some of which are located at the diencephalic–telencephalic boundary where *Emx2* has strong expression during development. These early developmental steps need to be considered to understand how altered *Emx2* expression leads to changes in the cortical targets.

ACKNOWLEDGMENTS

We thank Prof. Sharon Juliano, Ms. Courtney C. J. Voelker, and Ms. Lynden Guiver for thoughtful comments on the article; and Dr. Nadia Liapi, Dr. Luca Muzio, and Dr. Jose Miguel Soria for help with breeding and genotyping some of the mice used in this work. Z.M. and J.P. received funding from The Welcome Trust.

LITERATURE CITED

Allendoerfer KL, Shatz CJ. 1994. The subplate, a transient neocortical structure: its role in the development of connections between thalamus and cortex. Annu Rev Neurosci 17:185–218.

Bishop KM, Goudreau G, O'Leary DD. 2000. Regulation of area identity in mammalian neocortex by *Emx2* and *Pax6*. Science 288:344–349.

Blakemore C, Molnár Z. 1990. Factors involved in the establishment of specific interconnections between thalamus and cerebral cortex. Cold Spring Harb Symp Quant Biol 55:491–504.

Bolz J, Gotz M, Hubener M, Novak N. 1993. Reconstructing cortical connections in a dish. Trends Neurosci 16:310–316.

Catalano SM, Shatz CJ. 1998. Activity-dependent cortical target selection by thalamic axons. Science 281:559–562.

Catalano S, Robertson RT, Killackey HP. 1991. Early ingrowth of thalamocortical afferents to the neocortex of the prenatal rat. Proc Natl Acad Sci U S A 88:2999–3003.

Catalano SM, Robertson RT, Killackey HP. 1996. Individual axon morphology and thalamocortical topography in developing rat somatosensory cortex. J Comp Neurol 367:36–53.

De Carlos JA, O'Leary DD. 1992. Growth and targeting of subplate axons and establishment of major cortical pathways. J Neurosci 12:1194–1211.

Denaxa M, Chan CH, Schachner M, Parnavelas JG, Karagogeos D. 2001. The adhesion molecule TAG-1 mediates the migration of cortical interneurons from the ganglionic eminence along the corticofugal fiber system. Development 128:4635–4644.

Erzurumlu RS, Jhaveri S. 1992. Emergence of connectivity in the embryonic rat parietal cortex. Cereb Cortex 2:336–352.

Fernandez AS, Pieau C, Repérant J, Boncinelli E, Wassef M. 1998. Expression of the *Emx-1* and *Dlx-1* homeobox genes define three molecularly distinct domains in the telencephalon of mouse, chick, turtle and frog embryos: implications for the evolution of telencephalic subdivisions in amniotes. Development 101:2099–2111.

Fukuda T, Kawano H, Ohyama K, Li HP, Takeda Y, Oohira A, Kawamura K. 1997. Immunohistochemical localization of neurocan and L1 in the formation of thalamocortical pathway of developing rats. J Comp Neurol 382:141–152.

Gao PP, Yue Y, Zhang JH, Cerretti DP, Levitt P, Zhou R. 1998. Regulation of thalamic neurite outgrowth by the Eph ligand ephrin-A5: implications in the development of thalamocortical projections. Proc Natl Acad Sci U S A 95:5329–5334.

Godement P, Salaun J, Metin C. 1987. Fate of uncrossed retinal projections following early or late prenatal monocular enucleation in the mouse. J Comp Neurol 255:97–109.

Godfraind C, Schachner M, Goffinet AM. 1988. Immunohistochemical localization of cell adhesion molecules L1, J1, N-CAM and their common carbohydrate L2 in the embryonic cortex of normal and *reeler* mice. Dev Brain Res 42:99–111.

Gulisano M, Broccoli V, Pardini C, Boncinelli E. 1996. Emx1 and Emx2 show different patterns of expression during proliferation and differentiation of the developing cerebral cortex in the mouse. Eur J Neurosci 8:1037–1050.

Hevner RF, Miyashita E, Martin G, Rubenstein JLR. 1998. Lack of thalamocortical connections in mutants affecting cortical (TBR-1) or thalamic (GBX-2) gene expression. Soc Neurosci Abstr 24:58.

Hevner RF, Shi L, Justice N, Hsueh Y, Sheng M, Smiga S, Bulfone A, Goffinet AM, Campagnoni AT, Rubenstein JL. 2001. *Tbr1* regulates differentiation of the preplate and layer 6. Neuron 29:353–366.

Kawano H, Fukuda T, Kubo K, Horie M, Uyemura K, Takeuchi K, Osumi N, Eto K, Kawamura K. 1999. Pax-6 is required for thalamocortical pathway formation in fetal rats. J Comp Neurol 408:147–160.

Krettek JE, Price JL. 1977. The cortical projections of the mediodorsal nucleus and adjacent thalamic nuclei in the rat. J Comp Neurol 171:157–191.

Liu FC, Graybiel AM. 1992. Transient calbindin-D28K-positive systems in the telencephalon: ganglionic eminence, developing striatum and cerebral cortex. J Neurosci 12:674–690.

Leighton PA, Mitchell KJ, Goodrich LV, Lu X, Pinson K, Scherz P, Skarnes

WC, Tessier-Lavigne M. 2001. Defining brain wiring patterns and mechanisms through gene trapping in mice. Nature 410:174–179.

Levitt P. 1984. A monoclonal antibody to limbic system neurons. Science 223:299–301.

Mallamaci A, Iannone R, Briata P, Pintonello L, Mercurio S, Boncinelli E, Corte G. 1998. EMX2 protein in the developing mouse brain and olfactory area. Mech Dev 77:165–172.

Mallamaci A, Mercurio S, Muzio L, Cecchi C, Pardini CL, Gruss P, Boncinelli E. 2000a. The Lack of Emx2 causes impairment of reelin signaling and defects of neuronal migration in the developing cerebral cortex. J Neurosci 20:1109–1118.

Mallamaci A, Muzio L, Chan CH, Parnavelas J, Boncinelli E. 2000b. Area identity shifts in the early cerebral cortex of *Emx2*$^{-/-}$ mutant mice. Nat Neurosci 3:679–686.

Mann F, Zhukareva V, Pimenta A, Levitt P, Bolz J. 1998. Membrane-associated molecules guide limbic and nonlimbic thalamocortical projections. J Neurosci 18:9409–9419.

Marin O, Baker J, Puelles L, Rubenstein JL. 2002. Patterning of the basal telencephalon and hypothalamus is essential for guidance of cortical projections. Development 129:761–773.

McConnell SK, Ghosh A, Shatz CJ. 1989. Subplate neurons pioneer the first axon pathway from the cerebral cortex. Science 245:978–982.

Métin C, Godement P. 1996. The ganglionic eminence may be an intermediate target for corticofugal and thalamocortical axons. J Neurosci 16:3219–3235.

Mitrofanis J, Guillery RW. 1993. New views of the thalamic reticular nucleus in the adult and developing brain. Trends Neurosci 16:240–245.

Molnár Z. 1998. Development of thalamocortical connections. Berlin: Springer-Verlag.

Molnár Z. 2000. Conserved developmental algorithms during thalamocortical circuit formation in mammals and reptiles. In: Block G, editor. The developmental evolutionary biology of the cerebral cortex. Chichester: Wiley. p 148–172.

Molnár Z, Blakemore C. 1995. How do thalamic axons find their way to the cortex? Trends Neurosci 18:389–397.

Molnár Z, Butler AB. 2002. The corticostriatal junction: a crucial region for forebrain development and evolution. Bioessays 24:530–541.

Molnár Z, Cordery PM. 1999. Connections between cells of the internal capsule, thalamus and cerebral cortex in embryonic rat. J Comp Neurol 413:1–25.

Molnár Z, Hannan A. 2000. Development of thalamocortical projections in normal and mutant mice. In: Goffinet A, Rakic P, editors. Mouse brain development. Berlin: Springer-Verlag. p 293–332.

Molnár Z, Adams R, Blakemore C. 1998a. Mechanisms underlying the establishment of topographically ordered early thalamocortical connections in the rat. J Neurosci 18:5723–5745.

Molnár Z, Adams R, Goffinet AM, Blakemore C. 1998b. The role of the first postmitotic cells in the development of thalamocortical fiber ordering in the *reeler* mouse. J Neurosci 18:5746–5785.

Molnár Z, Knott GW, Blakemore C, Saunders NR. 1998c. Development of thalamocortical projections in the south American grey short-tailed Opossum (*Monodelphis Domestica*). J Comp Neurol 398:491–514.

Pellegrini M, Mansouri A, Simeone A, Boncinelli E, Gruss P. 1996. Dentate gyrus formation requires Emx2. Development 122:3893–3898.

Puelles L, Kuwana E, Puelles E, Bulfone A, Shimamura K, Keleher J, Smiga S, Rubenstein JL. 2000. Pallial and subpallial derivatives in the embryonic chick and mouse telencephalon, traced by the expression of the genes Dlx-2, Emx-1, Nkx-2.1, Pax-6, and Tbr-1. J Comp Neurol 424:409–438.

Rakic P. 1977. Prenatal development of the visual system in the rhesus monkey. Philos Trans R Soc Lond B Biol Sci 278:245–260.

Robertson RT, Kaitz SS. 1981. Thalamic connections with limbic cortex. I. Thalamocortical projections. J Comp Neurol 195:501–525.

Simeone A, Acampora D, Gulisano M, Stornaiuolo A, Boncinelli E. 1992a. Nested expression domains of four homeobox genes in developing rostral brain. Nature 358:687–690.

Simeone A, Gulisano M, Acampora D, Stornaiuolo A, Rambaldi M, Boncinelli E. 1992b. Two vertebrate homeobox genes related to the Drosophila empty spiracles gene are expressed in the embryonic cerebral cortex. EMBO J 11:2541–2550.

Stoykova A, Gruss P. 1994. Roles of Pax-genes in developing and adult brain as suggested by expression patterns. J Neurosci 14:1395–1412.

Stoykova A, Treichel D, Hallonet M, Gruss P. 2000. Pax6 modulates the dorsoventral patterning of the mammalian telencephalon. J Neurosci 20:8042–8050.

Suda Y, Hossain ZM, Kobayashi C, Hatano O, Yoshida M, Matsuo I, Aizawa S. 2001. Emx2 directs the development of diencephalon in cooperation with Otx2. Development 128:2433–2450.

Takemoto M, Fukuda T, Murakami F, Tanaka H, Yamamoto N. 2001. The role of Ephrin-B3 in the formation of region- and lamina-specific thalamocortical projections. Neurosci Res Suppl 24:S136.

Tole S, Goudreau G, Assimacopoulos S, Grove EA. 2000. Emx2 is required for growth of the hippocampus but not for hippocampal field specification. J Neurosci 20:2618–2625.

Tuttle R, Nakagawa Y, Johnson JE, O'Leary DD. 1999. Defects in thalamocortical axon pathfinding correlate with altered cell domains in Mash-1-deficient mice. Development 126:1903–1916.

Yamamoto M, Boyer AM, Crandall JE, Edwards M, Tanaka H. 1986. Distribution of stage-specific neurite-associated proteins in the developing murine nervous system recognized by a monoclonal antibody. J Neurosci 6:3576–3594.

Yoshida M, Suda Y, Matsuo I, Miyamoto N, Takeda N, Kuratani S, Aizawa S. 1997. Emx1 and Emx2 functions in development of dorsal telencephalon. Development 124:101–111.